A Study of a Boundary Value Problem and Its Equivalent Fredholm / Volterra Integral Equation Formulation

A PROJECT REPORT

SUBMITTED IN PARTIAL FULFILLMENT OF THE COMPLETION OF MINOR REPORT IN THE DEGREE

Master of Science
in
Applied Mathematics

Submitted by

SUDHANSHU RANJAN (24/MSCMAT/09)

Under the supervision of

Dr.Vivek Kumar Aggarwal

Department of Applied Mathematics

DELHI TECHNOLOGICAL UNIVERSITY

(Formerly Delhi College of Engineering)

Bawana Road, Delhi 110042

MAY, 2026

DEPARTMENT OF APPLIED MATHEMTICS
DELHI TECHNOLOGICAL UNIVERSITY

(Formerly Delhi College of Engineering)

Bawana Road, Delhi-110042

CANDIDATE'S DECLARATION

I, **SUDHNSHU RANJAN**, Roll No:-**24/MSCMAT/09** students of **MSc (Applied Mathematics)**, hereby declare that the project Dissertation titled **"A Study of a Boundary Value Problem and Its Equivalent Fredholm / Volterra Integral Equation Formulation"** which is submitted by us to the Applied Mathematics, Delhi Technological University, Delhi in partial fulfilment of the requirement for the award of degree of Master's of Science, is original and not copied from any source without proper citation. This work has not previously formed the basis for the award of any Degree, Diploma Associateship, Fellowship or other similar title or recognition.

Place: Delhi **Sudhanshu Ranjan**

Date: 23.05.26

DEPARTMENT OF APPLIED MATHEMATICS
DELHI TECHNOLOGICAL UNIVERSITY

(Formerly Delhi College of Engineering)

Bawana Road, Delhi-110042

CERTIFICATE

I hereby certify that the Project Dissertation titled **"A Study of a Boundary Value Problem and Its Equivalent Fredholm / Volterra Integral Equation Formulation"** which is submitted by **Sudhanshu Ranjan**, Roll No:- **24/MSCMAT/09**, **Department of Applied Mathematics**, Delhi Technological University, Delhi in partial fulfilment of the requirement for the award of the degree of Master's Of Science, is a record of the project work carried out by the students under my supervision. To the best of my knowledge this work has not been submitted in part or full for any Degree or Diploma to this University or elsewhere.

Place: Delhi

Date: 26.05.2026

Dr. Vivek Kumar Aggarwal

SUPERVISOR

DEPARTMENT OF APPLIED MATHEMATICS
DELHI TECHNOLOGICAL UNIVERSITY

(Formerly Delhi College of Engineering)

Bawana Road, Delhi-110042

ACKNOWLEDGEMENT

I wish to express our sincerest gratitude to **Dr.Vivek Kumar Aggarwal** for his continuous guidance and mentorship that he provided us during the project. He showed us the path to achieve our targets by explaining all the tasks to be done and explained to us the importance of this project as well as its industrial relevance. He was always ready to help us and clear our doubts regarding any hurdles in this project. Without his constant support and motivation, this project would not have been successful.

Place: Delhi **Sudhanshu Ranjan**

Date: 23.05.2026

Abstract

This dissertation presents a comprehensive study of linear second-order boundary value problems (BVPs) and their equivalent integral formulations. The model differential equation

$$u''(x) = x + 1, \quad 0 \le x \le 1, \quad u(0) = 0,\ u(1) = 0$$

is first solved analytically using classical ordinary differential equation techniques. The corresponding Green's function for the differential operator is then derived, allowing the reformulation of the BVP as a Fredholm integral equation of the second kind.

In addition, a singularly perturbed boundary value problem of the form

$$\varepsilon u''(x) + a(x)\, u'(x) + b(x)\, u(x) = f(x), \quad u(0) = u_0,\ u(1) = u_1$$

is considered, where ε is a small positive parameter. The study examines the behavior of the solution under perturbation and investigates whether the solution obtained from the differential equation is equivalent to its corresponding integral equation formulation.

Both analytical and numerical methods are employed to evaluate the integral representations, and the resulting solutions are shown to be consistent with those obtained from the differential equations. All the numerical calculations in this paper were carried out in MATLAB using the solution of boundary value problems by numerical quadrature of the Fredholm integral equation, finite difference approximations and `bvp4c`,in solving ordinary differential equations. Comparison graphs between exact solution and numerical solutions from ODE and integral equation showed that their results agreed very well within the error of order of machine precision.

We have showed that solutions of a boundary value problem posed in the form of differential equation and that posed in the form of integral equation agreed well when proper condition exists even in singular perturbation case, and that Green function can be a tool to transform boundary value problems into tractable integral equations

Contents

List of Figures

List of Tables

List of Nomenclature

Roman Symbols

$u(x)$	Solution of the boundary value problem
$u'(x)$	First derivative of u with respect to x
$u''(x)$	Second derivative of u with respect to x
$u_0(x)$	Outer (reduced) solution
$u_1(x)$	First-order outer correction
$u_p(x)$	Particular integral / particular solution
$u_h(x)$	Homogeneous (complementary) solution
$u_{comp}(x)$	Composite uniformly valid approximation
u_{ODE}	Solution obtained via differential equation method
u_{IE}	Solution obtained via integral equation method
$v(\xi)$	Inner (boundary-layer) solution in stretched variable
$v_0(\xi)$	Leading-order inner solution
$G(x,s)$	Green's function for the differential operator L
$G(x,t)$	Green's function for the operator L_ε
$G_0(x,t)$	Green's function for the operator $L_0 = \varepsilon D^2 + a(x)D$
$H(x)$	Harmonic interpolant / lifting function
$h(x)$	Source-free interpolant satisfying boundary conditions
$K(x,s)$	Kernel of the Fredholm integral equation
L	Linear differential operator
L_ε	Singularly perturbed differential operator $\varepsilon D^2 + a(x)D + b(x)I$
L_0	Reduced operator $\varepsilon D^2 + a(x)D$
L_ε^*	Adjoint operator of L_ε
$W(x)$	Wronskian of homogeneous solutions
$W(t)$	Wronskian evaluated at t
$f(x)$	Forcing / source function (right-hand side)
$f_0(x)$	Free term in the Fredholm integral equation
$a(x)$	Coefficient of $u'(x)$ in the differential equation
$b(x)$	Coefficient of $u(x)$ in the differential equation
T	Fredholm integral operator
T^n	n-th iterate of the Fredholm integral operator
$\varphi_1(x)$	First homogeneous solution satisfying $\varphi_1(0) = 0$
$\varphi_2(x)$	Second homogeneous solution satisfying $\varphi_2(1) = 0$
C_1, C_2	Constants of integration
U_0	Boundary value at $x = 0$

U_1	Boundary value at $x = 1$
A_0, B_0	Constants in leading-order inner solution
λ_1	Slow (outer) characteristic root
λ_2	Fast (boundary-layer) characteristic root
N	Number of mesh points / subintervals
h	Mesh step size $h = 1/N$
x_i	i-th mesh point $x_i = ih$
$E[u]$	Energy functional $\displaystyle\int_0^1 (u')^2\,dx$
$F(x)$	Integral $\displaystyle\int_0^x e^{s^2/2}\sin s\,ds$ (Example 2 outer solution)
$M(x)$	Integral $\displaystyle\int_0^x \frac{e^s}{\cos s}\,ds$ (Example 3 integrating factor exponent)
$\Phi(x)$	Integral $\displaystyle\int_0^x e^{-\sin(s)/\varepsilon}\,ds$ (Example 3 fundamental solution)
$\Psi(x)$	Integral $\displaystyle\int_0^x e^{-(s+s^2/2)/\varepsilon}\,ds$ (Example 4 fundamental solution)
$\Lambda(\varepsilon)$	Normalising constant $\displaystyle\int_0^1 e^{-s^2/(2\varepsilon)}\,ds$ (Example 2)

Greek Symbols

ε	Small positive perturbation parameter, $\varepsilon \in (0, 1]$
ξ	Stretched (inner) coordinate $\xi = x/\varepsilon$ (or $\xi = x/\sqrt{\varepsilon}$ at turning points)
δ	Boundary layer thickness $\delta = \varepsilon/a(0)$
α_0	Lower bound on $a(x)$; $a(x) \geq \alpha_0 > 0$
$\mu(x)$	Integrating factor of the reduced equation
$\delta(x - s)$	Dirac delta distribution centred at s
$\rho(T)$	Spectral radius of the integral operator T
λ	Eigenvalue / characteristic root

Mathematical Abbreviations and Notation

BVP	Boundary Value Problem
ODE	Ordinary Differential Equation
IE	Integral Equation
MAE	Matched Asymptotic Expansion
WKB	Wentzel–Kramers–Brillouin (semiclassical approximation)
erf	Error function $\operatorname{erf}(z) = \frac{2}{\sqrt{\pi}} \int_0^z e^{-t^2}\, dt$
$C^2[0,1]$	Space of twice continuously differentiable functions on $[0,1]$
$C[0,1]$	Space of continuous functions on $[0,1]$
$\|\cdot\|_\infty$	Supremum (maximum) norm
$\|\cdot\|_{L^1}$	L^1 norm
$O(\varepsilon)$	Big-O notation; bounded by a constant multiple of ε as $\varepsilon \to 0$
δ_{ij}	Kronecker delta
Re	Reynolds number
Pe	Péclet number
bvp4c	MATLAB collocation solver for boundary value problems

Chapter 1

Introduction

Boundary value problems (BVPs) appear ubiquitously in physical, engineering, and mathematical modeling phenomena such as heat conduction, mechanical vibrations, fluid flow, electrostatics, quantum mechanics, etc. Fundamentally, a BVP consists of a differential equation and boundary conditions specifying certain behavior on the boundary of the region or domain of interest. BVPs differ from initial value problems in that initial value problems give all information required to solve the problem at a single point whereas BVPs require that the solution must satisfy some condition or set of conditions at two or more points. HenceBVPs generally require more sophisticated analysis and numerical techniques than their counterparts. One approach to analyzingBVPs is by direct investigation of the boundary value differential equation using concepts from calculus, linear algebra, and differential equations. However, many boundary value problems may also be formulated as boundary value integral equations (typically either Fredholm or Volterra types). The alternative integral formulation enjoys several advantages, such as enabling a deeper theoretical analysis of the problem, providing an alternative approach for the development of numerical schemes and highlighting fundamental structure of underlying operators. A critical part of this formulation requires derivation of the appropriate Green's function, which accounts for the effect of the boundary conditions on the problem at hand and represents the differential equation as an equivalent integral representation. In this dissertation we will consider both the theoretical and numerical equivalency between a boundary value problem and its integral equation counterpart. We will analyze two model problems. The first problem we consider is: The second order linear boundary value problem

$$u''(x) = x + 1, \quad 0 \leq x \leq 1, \quad u(0) = 0,\ u(1) = 0,$$

Which can be solved analytically using standard ODE techniques and rephrased as a Fredholm second kind integral equation with its Green's function. The other alternative

model problem,

$$y''(x) + 2y(x) = x, \quad y(0) = 1,\ y(1) = 0,$$

is incorporated to showcase the wider relevance of the approach and to confirm the equivalence through an independent example.For both cases, the analytical solution to the ODEs are shown to agree with those determined from their associated integral equations. Apart from the analytical solutions, numerical methods are also an indispensable part of this investigation.The problems are implemented using MAT LAB where solutions to BVPs and integral equations are approximated using *bvp4c*, trapezoidal quadrature rule and finite difference method. The latter part of this dissertation extends the study to a more demanding class of problems: *singularly perturbed* second-order boundary value problems of the form

$$\varepsilon\, u''(x) + a(x)\, u'(x) + b(x)\, u(x) = f(x), \quad 0 \le x \le 1, \quad u(0) = U_0,\ u(1) = U_1,$$

where $\varepsilon \in (0, 1]$ is a small positive parameter For $= 1$, although in most regions of the domain the coefficient of the highest-order derivative is of negligible magnitude, it qualitatively alters the nature of the problem; we obtain a boundary layer, a thin region of large gradient variation of thickness O(/a(0)) near x = 0 (where a(x) > 0), which cannot be approximated with $= 0$. Many different problems in physics appear of this type, such as high Reynolds number fluid flow (Prandtl boundary layers), advection-dominant heat transfer (high Peclet number), the semiclassical limit of quantum mechanics (WKB approximation), and cheap-control problems in the optimal control theory. Two distinct methods help in analyzing them. *Matched asymptotic expansions* decompose the solution into an outer region, governed by the reduced first-order equation obtained by setting $\varepsilon = 0$, and an inner boundary-layer region, described by a rescaled equation in the stretched coordinate $\xi = x/\varepsilon$; the two are joined via asymptotic matching to yield a composite approximation that is uniformly valid on the entire interval. Independently, the *Green's function approach* reformulates each singularly perturbed BVP as a Fredholm integral equation of the second kind, embedding the boundary conditions into the kernel and converting the stiff differential problem into a compact integral operator whose Neumann series converges rapidly for small ε. Five representative examples—spanning constant coefficients, turning-point (degenerate) problems, trigonometric and exponential variable coefficients, and an exact-differential structure—are worked out in full, their integral equation formulations are constructed explicitly, and the two approaches are shown to yield identical solutions, in agreement with the general equivalence theorem proved in Chapter 13.Each of the approaches is explored, noting the computational pros and cons, memory demands, condition number and layer-adapted meshes.

In this dissertation we have then a twofold goal: (i) a clean and systematic derivation

of the integral equation formulations that represent a linear BVP, (ii) comparing the results derived analytically, by solving it via the integral equation or numerically, via computational experiments. The answer seems to prove the two formulas are the same, and display the Green function method to solve BVP.

Chapter 2

Literature Review

2.1 Boundary Value Problems: Classical Theory and Solution Methods

Second-order linear boundary value problems (BVPs) can be considered among the most well-understood classes of ordinary differential equations. A general second-order linear BVP can be stated in the form

$$a(x)u''(x) + b(x)u'(x) + c(x)u(x) = f(x), \quad x \in (a, b) \tag{2.1}$$

with appropriate boundary conditions defining values or derivatives of the solution at two or more distinct points. In opposition to initial value problems in which all of the data is known at a single point, the analysis and computation associated with boundary value problems are more complicated since the problem entails solving for an entity that is constrained by multiple points of data simultaneously. In cases where the differential operator involved has constant coefficients, existence and uniqueness are immediately implied by the characteristic equation; indeed, homogeneous solutions can be found using the roots λ_1, λ_2, while particular solutions may be found either via the method of undetermined coefficients or variation of parameters. For operators of variable coefficient type, such as the Airy or Bessel problems, the corresponding homogeneous solutions involve special functions and, consequently, a greater variety of solutions will exist. The existence and uniqueness of solutions to variable-coefficient BVPs will be ensured provided that the operator L meets some basic criteria; namely, the leading coefficient must not vanish, and the operator satisfies a maximum principle, i.e., that there exists a bound on the operator independent of the [28, 11]. As an example, consider the simple uniqueness theorem for the operator $L[u] = u''$ with homogeneous Dirichlet conditions on $[0, 1]$,

namely $u(0) = u(1) = 0$; here, the general solution is clearly

$$u(x) = C_1 x + C_2, \tag{2.2}$$

from which the boundary conditions yield $C_1 = C_2 = 0$. Thus the only possible solution is $u = 0$. An energy argument also shows this, since

$$\int_0^1 (u')^2 \, dx = 0$$

and so $u' = 0$, which implies that u is constant. The boundary conditions would then make $u = 0$. This technique may easily be generalized to operators of higher order and for PDEs.

2.2 Green's Functions and Integral Equation Reformulations

2.2.1 Green's Function Theory

The Green's function $G(x, s)$, associated with a linear operator L along with boundary conditions, is used to represent the response of the system due to a delta source. This is because it fulfills the condition

$$L[G(\cdot, s)](x) = \delta(x - s)$$

subject to the prescribed boundary conditions.

Once the Green's function is found, the solution to

$$L[u] = f$$

is expressed as

$$u(x) = \int_a^b G(x, s) f(s) \, ds,$$

and thus converts the differential equation with boundary conditions into an integral evaluation. For the operator $L[u] = u''$ on $[0, 1]$ with $u(0) = u(1) = 0$, the Green's function is piecewise linear:

$$G(x, s) = \begin{cases} (1 - s)\, x, & 0 \le x \le s, \\ s\,(1 - x), & s \le x \le 1. \end{cases}$$

The basis is that we enforce G continuous at x = s and that it have a unit jump in G/x at the source. For detail explanations of the construction and examples, we refer the reader to Stakgold and Holst [28] and Kress [11]. We know that, for self-adjoint operators, we have a systematic construction for such kernels using the Sturm-Liouville theory.

2.2.2 Fredholm and Volterra Integral Equations

The reformulation of BVPs into integral equations is one of the classic powerful strategies. There are two main classes of integral equations: Fredholm integral equations, in which the interval of integration isfixed [a, b]; and Volterra integral equations, in which the upper limit of integration is the variable x. The Green's function representation leads to a Fredholm integral equation of the second kind for the stationary BVP:

$$u(x) = f(x) + \lambda \int_a^b K(x,s)\, u(s)\, ds,$$

When $K(x,s)$ is dependent upon green's function and coefficient $b(x)$ of original operator. Symmetry, compactness and spectral components of the kernel's structure are passed down directly from the original differential operator and compactness on $C[0,1]$ of the integral operator (via Arzelà-Ascoli's Theorem) ensures convergence of Galerkin, collocation and Nyström discretisations without regard to any stiffness in the original ODE: [11].

Volterra equations are often the result of modeling problems with a memory or history characteristic, for example initial value problems and causal systems. Much analysis can be found in the literature discussing discretisation methods for both categories; the continuity of the kernel strongly affects both stability and conditioning. Thus smooth kernels allow for quadrature formulas of high order, while for weakly singular kernels special weight-corrected rules are necessary [12, 17].

2.3 Singularly Perturbed Boundary Value Problems

2.3.1 Mathematical Framework and Boundary Layer Phenomena

A singularly perturbed BVP arises when a small positive parameter ε multiplies the highest-order derivative:

$$\varepsilon\, u''(x) + a(x)\, u'(x) + b(x)\, u(x) = f(x), \quad u(0) = U_0, \quad u(1) = U_1.$$

If we set $\varepsilon = 0$ in which the equation degenerates into first-order (i.e.) the *reduced problem* $a(x)\, u0' + b(x)\, u0 = f(x)$ has only one of the two boundary conditions satisfied. The jump

at the other endpoint is accommodated by a *boundary layer* which is a narrow strip of thickness $O(\varepsilon/a(0))$ around $x = 0$ (when $a(x) > 0$), where $u(x)$ transitions abruptly from U_0 to $u(x)$, the slowly varying function in the outside region. The following analysis depends on such two-scale problem. [15, 10, 14].

An ε-uniform stability bound of the form

$$\|u\|_\infty \le \max\{|U_0|, |U_1|\} + \frac{1}{\alpha_0}\|f\|_\infty, \qquad |u'(x)| \le C_1\big(1 + \varepsilon^{-1}e^{-\alpha_0 x/\varepsilon}\big)$$

can be established under the assumption $a(x) \ge \alpha_0 > 0$, quantifying the rapid exponential variation inside the layer. Such estimates, proved via maximum-principle arguments and barrier functions, are standard in the literature on ε-uniform numerical methods [12, 17].

2.3.2 Matched Asymptotic Expansions

The approach of matched asymptotic expansions splits the solution into an outer region (u 0 and the reduced equation applies) and an inner (boundary layer) region in which the stretched variable = x/ can be used so as to put the second-derivative term back at leading order. The leading inner equation $v_0'' + a(0)\,v_0' = 0$ has solution $v_0(\xi) = A_0 + B_0 e^{-a(0)\xi}$, and the matching condition as $\xi \to \infty$ requires $A_0 = u_0(0)$, so $B_0 = U_0 - u_0(0)$. The composite uniformly valid approximation

$$u_{\text{comp}}(x) = u_0(x) + \big(U_0 - u_0(0)\big)\, e^{-a(0)x/\varepsilon} + O(\varepsilon)$$

captures both regimes in a single closed-form formula, with $O(\varepsilon)$ error in the supremum norm [2, 20, 21].At *turning points*, where $a(x_0) = 0$ at some interior or boundary point, the standard $O(\varepsilon)$ layer width is replaced by $O(\sqrt{\varepsilon})$, the inner equation becomes the Weber (parabolic cylinder) equation, and the inner solution is expressed in terms of the error function rather than a pure exponential. This case requires modified WKB analysis and the theory of Stokes phenomena [22, 2].

2.3.3 Applications and Numerical Methods

Singularly perturbed convection–diffusion equations arise in a wide range of physical contexts: Prandtl's boundary layer equations in fluid mechanics at high Reynolds number [16], steady-state advection–diffusion in heat transfer at high Péclet number, the semiclassical (WKB) limit of the Schrödinger equation in quantum mechanics, the cheap-control limit of linear-quadratic optimal control problems, and concentration profiles in stiff reaction–diffusion systems[?][?]. In each case, the parameter ε represents a ratio of length scales (diffusive to advective or quantum to classical), and the boundary layer is the mathematical counterpart of a thin physical transition zone.

As far as the numerical approach goes, ordinary finite difference schemes on uniform meshes generate false oscillations whenever h>, which are to be suppressed by upwinding [1, 7] or employing meshes adapted to the boundary layers, such as Shishkin or Bakhvalov meshes [18]. Collocation solvers such as MATLAB's `bvp4c` address stiffness by constructing global polynomial approximations with residual control [17]. The integral equation framework offers a complementary advantage: the Green's function kernel smooths the sharp layer structure, enabling uniform convergence on coarse meshes without mesh adaptation, and the Fredholm operator's compactness yields convergence of the Neumann series at rate $O(\varepsilon^n)$ per iteration in non-turning-point problems [11, 28].

Work on fitted mesh B-spline collocation by Kadalbajoo and Aggarwal [8] demonstrates that carefully designed basis functions can resolve boundary layers without the exponentially large condition numbers that af[**?**, **?**, **?**, **?**, **?**]flict uniform-mesh finite differences. The present dissertation contributes by demonstrating—both analytically and numerically—the full equivalence of the differential and integral formulations for a representative set of model problems, implementing and comparing `bvp4c`, Fredholm quadrature, and finite difference schemes, and providing reproducible MATLAB code as pedagogical benchmarks.

Chapter 3

Preliminaries on Boundary Value Problems

3.1 Second–Order Linear BVPs

We consider linear second-order boundary value problems of the general form

$$\begin{cases} L[u](x) := a(x)u''(x) + b(x)u'(x) + c(x)u(x) = f(x), \quad a < x < b, \\ \alpha_1 u(a) + \beta_1 u'(a) = \gamma_1, \\ \alpha_2 u(b) + \beta_2 u'(b) = \gamma_2, \end{cases} \tag{3.1}$$

where $a(x)$, $b(x)$, $c(x)$, and $f(x)$ are given functions and $\alpha_i, \beta_i, \gamma_i$ are constants specifying the boundary conditions.

In this work, we focus on the simplest case of Dirichlet boundary conditions for the operator

$$L[u](x) = u''(x),$$

with $u(0) = 0$ and $u(1) = 0$.

3.2 Existence and Uniqueness

We recall a standard result for the simple operator $L[u] = u''$.

Theorem 3.1 (Uniqueness for the Homogeneous Problem)**.** *Consider the homogeneous BVP*

$$u''(x) = 0, \quad 0 \le x \le 1, \quad u(0) = 0,\ u(1) = 0.$$

Then the only solution is $u(x) \equiv 0$.

Proof. The general solution of $u''(x) = 0$ is

$$u(x) = C_1 x + C_2,$$

where C_1, C_2 are constants. Applying the boundary conditions,

$$u(0) = C_2 = 0, \qquad u(1) = C_1 + C_2 = C_1 = 0.$$

Hence $C_1 = C_2 = 0$ and therefore $u(x) \equiv 0$. □

Theorem 3.1 implies that any inhomogeneous BVP with $u''(x) = f(x)$ and the same boundary conditions has at most one solution.

Physical Interpretation. Equation $u'' = 0$ describes zero acceleration. A function with zero acceleration moves with constant velocity — a straight line. If you pin both ends at zero, the string must lie flat. So the only physical solution is rest-state displacement $u \equiv 0$.

Energy Argument. Define the energy-like functional

$$E[u] = \int_0^1 \big(u'(x)\big)^2 \, dx.$$

Since $u'' = 0$, integration by parts gives

$$E[u] = -\int_0^1 u(x)\, u''(x)\, dx = 0.$$

Thus

$$\int_0^1 (u')^2 \, dx = 0 \implies u' = 0 \implies u = \text{constant}.$$

Applying the boundary conditions yields $u = 0$. This method generalises to higher-order PDEs.

Chapter 4

Green's Functions for Second–Order BVPs

4.1 Definition

Let L be a linear differential operator and consider the BVP

$$L[u](x) = f(x), \quad a < x < b,$$

together with suitable boundary conditions. A Green's function $G(x, s)$ associated with L and the boundary conditions is a function satisfying:

1. For each fixed s, $G(\cdot, s)$ satisfies the homogeneous equation $L[G(\cdot, s)] = 0$ for $x \neq s$.
2. $G(x, s)$ satisfies the given boundary conditions as a function of x.
3. $G(x, s)$ has a specific jump condition in its first derivative at $x = s$ which enforces

$$L[G(\cdot, s)] = \delta(x - s)$$

in a distributional sense.

Once the Green's function is known, the solution can often be written as

$$u(x) = \int_a^b G(x, s)\, f(s)\, ds. \tag{4.1}$$

4.2 Green's Function for u'' with Dirichlet BCs

We now construct the Green's function for the operator $L[u] = u''(x)$ on $[0, 1]$ with $u(0) = 0$, $u(1) = 0$.

We seek $G(x,s)$ such that:

$$\frac{\partial^2 G}{\partial x^2}(x,s) = \delta(x-s), \quad 0 < x < 1,$$

with $G(0,s) = 0$, $G(1,s) = 0$.

For fixed $s \in (0,1)$, the function $x \mapsto G(x,s)$ is piecewise linear:

$$G(x,s) = \begin{cases} A_1(s)\,x + B_1(s), & 0 \le x \le s, \\ A_2(s)\,x + B_2(s), & s \le x \le 1. \end{cases}$$

From the boundary conditions:

$$G(0,s) = B_1(s) = 0, \qquad G(1,s) = A_2(s) + B_2(s) = 0.$$

Continuity at $x = s$ gives

$$A_1(s)\,s + B_1(s) = A_2(s)\,s + B_2(s).$$

The jump condition on the first derivative is

$$\frac{\partial G}{\partial x}(s^+,s) - \frac{\partial G}{\partial x}(s^-,s) = 1, \quad \text{i.e.} \quad A_2(s) - A_1(s) = 1.$$

Solving these conditions yields

$$G(x,s) = \begin{cases} (1-s)\,x, & 0 \le x \le s, \\ s\,(1-x), & s \le x \le 1. \end{cases} \tag{4.2}$$

Chapter 5

Fredholm and Volterra Integral Equations

5.1 Fredholm Integral Equations

A Fredholm integral equation of the second kind has the general form

$$u(x) = f(x) + \lambda \int_a^b K(x,s)\, u(s)\, ds,$$

where $K(x,s)$ is called the kernel. In our problem, the integral equation obtained from the Green's function representation is of the form

$$u(x) = \int_0^1 G(x,s)\, f(s)\, ds,$$

which is a Fredholm equation with $\lambda = 0$ (pure representation formula).

5.2 Volterra Integral Equations

A Volterra integral equation of the second kind is of the form

$$u(x) = f(x) + \int_a^x K(x,s)\, u(s)\, ds.$$

Volterra equations naturally arise in problems with memory or hereditary effects. Although our main problem is more directly a Fredholm-type representation, the same philosophy of rewriting a differential equation as an integral equation applies.

Chapter 6

Formulation and Solution of the Model Problem

6.1 Differential Equation Solution

We consider again the BVP:

$$u''(x) = x + 1, \quad 0 \le x \le 1, \quad u(0) = 0,\ u(1) = 0.$$

First, we find the general solution of the differential equation. Integrating twice:

$$u''(x) = x + 1 \implies u'(x) = \int (x+1)\,dx = \frac{x^2}{2} + x + C_1,$$

$$u(x) = \int \left(\frac{x^2}{2} + x + C_1\right) dx = \frac{x^3}{6} + \frac{x^2}{2} + C_1 x + C_2,$$

for constants C_1, C_2. Applying boundary conditions:

$$u(0) = C_2 = 0, \qquad u(1) = \frac{1}{6} + \frac{1}{2} + C_1 = 0 \implies C_1 = -\frac{2}{3}.$$

Thus,

$$u(x) = \frac{x^3}{6} + \frac{x^2}{2} - \frac{2}{3}x = \frac{x^3 + 3x^2 - 4x}{6} = \frac{x(x^2 + 3x - 4)}{6}. \tag{6.1}$$

6.2 Integral Equation Formulation Using Green's Function

We now use the Green's function $G(x,s)$ constructed earlier (equation (4.2)). The right-hand side is $f(s) = s+1$. The solution is given by

$$u(x) = \int_0^1 G(x,s)\,(s+1)\,ds. \tag{6.2}$$

Because of the piecewise definition, we split the integral:

$$u(x) = \int_0^x s(1-x)(s+1)\,ds + \int_x^1 (1-s)\,x\,(s+1)\,ds.$$

First integral.

$$I_1(x) = \int_0^x s(1-x)(s+1)\,ds = (1-x)\int_0^x s(s+1)\,ds.$$

Computing the inner integral:

$$\int s(s+1)\,ds = \int (s^2+s)\,ds = \frac{s^3}{3} + \frac{s^2}{2}.$$

Thus

$$I_1(x) = (1-x)\left(\frac{x^3}{3} + \frac{x^2}{2}\right).$$

Second integral.

$$I_2(x) = \int_x^1 (1-s)\,x\,(s+1)\,ds = x\int_x^1 (1-s)(s+1)\,ds.$$

Note that $(1-s)(s+1) = 1-s^2$, so

$$\int (1-s^2)\,ds = s - \frac{s^3}{3}.$$

Hence

$$I_2(x) = x\left[\left(1-\frac{1}{3}\right) - \left(x - \frac{x^3}{3}\right)\right] = x\left(\frac{2}{3} - x + \frac{x^3}{3}\right).$$

Sum. A straightforward simplification yields

$$u(x) = I_1(x) + I_2(x) = \frac{x^3 + 3x^2 - 4x}{6},$$

which is exactly the same as in (6.1). Thus the integral formulation and the differential formulation are **equivalent** for this BVP.

6.3 Another Model Problem

Differential Equation Solution

We consider the BVP

$$y''(x) + 2y(x) = x, \quad 0 < x < 1, \quad y(0) = 1,\ y(1) = 0. \tag{6.3}$$

Homogeneous equation. The auxiliary equation $m^2 + 2 = 0$ gives $m = \pm i\sqrt{2}$, so

$$y_h(x) = A\cos(\sqrt{2}\,x) + B\sin(\sqrt{2}\,x).$$

Particular solution. Try $y_p = ax + b$. Then $y_p'' = 0$ and $2(ax+b) = x$, giving $a = 1/2$, $b = 0$, so $y_p(x) = x/2$.

Boundary conditions.

$$y(0) = 1 \implies A = 1.$$

$$y(1) = 0 \implies \cos(\sqrt{2}) + B\sin(\sqrt{2}) + \tfrac{1}{2} = 0 \implies B = -\frac{\cos(\sqrt{2}) + \frac{1}{2}}{\sin(\sqrt{2})}.$$

Final ODE solution.

$$y_{\text{ODE}}(x) = \cos(\sqrt{2}\,x) - \frac{\cos(\sqrt{2}) + \frac{1}{2}}{\sin(\sqrt{2})}\sin(\sqrt{2}\,x) + \frac{x}{2}. \tag{6.4}$$

6.4 Fredholm Integral Formulation and Comparison with ODE Solution

We consider the BVP (6.3).

6.4.1 Step 1: Reduction to Homogeneous Boundary Conditions

We write $g(x) = 2$, $h(x) = x$, $\alpha = y(0) = 1$, $\beta = y(1) = 0$. Define the lifting function $H(x) = \alpha + (\beta - \alpha)x = 1 - x$, and write $y(x) = u(x) + H(x)$, so that $u(0) = u(1) = 0$. Using

$$F(x) = h(x) - \alpha g(x) - (\beta - \alpha)x\,g(x),$$

we obtain $F(x) = x - 2 + 2x = 3x - 2$. The reduced problem is

$$u''(x) + 2u(x) = F(x) = 3x - 2, \quad u(0) = 0,\ u(1) = 0. \tag{6.5}$$

6.4.2 Step 2: Fredholm Integral Equation

Rewrite (9.2.1) as $u''(x) = 3x - 2 - 2u(x)$. The Green's function for u'' with homogeneous Dirichlet boundary conditions on $[0, 1]$ is

$$G(x,t) = \begin{cases} t(1-x), & 0 \le t \le x, \\ x(1-t), & x \le t \le 1. \end{cases} \tag{6.6}$$

Thus

$$u(x) = \int_0^1 G(x,t)\big(3t - 2 - 2u(t)\big)\,dt = f_0(x) - 2\int_0^1 G(x,t)\,u(t)\,dt,$$

where

$$f_0(x) = \int_0^1 G(x,t)(3t-2)\,dt = -\tfrac{1}{2}x(1-x)^2.$$

Hence the Fredholm equation is

$$u(x) = -\tfrac{1}{2}x(1-x)^2 - 2\int_0^1 G(x,t)\,u(t)\,dt, \tag{6.7}$$

and the full solution is

$$y(x) = u(x) + 1 - x. \tag{6.8}$$

6.4.3 Step 3: Comparison of Both Solutions

If u satisfies the Fredholm equation (6.7), then differentiating twice and using $\partial^2 G/\partial x^2 = \delta(x-t)$ gives $u''(x) = 3x - 2 - 2u(x)$, and by (6.8), $y(x) = u(x) + 1 - x$ satisfies

$$y''(x) + 2y(x) = x, \quad y(0) = 1,\ y(1) = 0.$$

By uniqueness, $y(x) = y_{\mathrm{ODE}}(x)$. Thus the Fredholm integral formulation and the ODE approach yield exactly the same solution.

Chapter 7

Numerical Simulations and Graphs

7.1 Graph of the Analytical Solution

Below we display the solution $u(x) = \dfrac{x^3 + 3x^2 - 4x}{6}$ on $[0, 1]$.

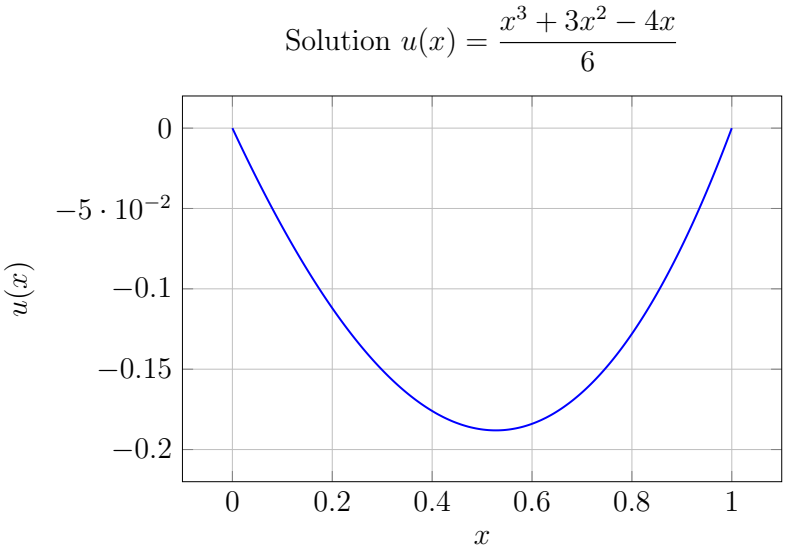

Figure 7.1: Analytical solution of the BVP $u''(x) = x + 1$, $u(0) = u(1) = 0$.

7.2 Remarks on Numerical Approximation

One may discretise the interval $[0, 1]$ into a uniform grid and approximate the second derivative using finite differences, or approximate the integral representation (6.2) using numerical quadrature (e.g., the composite trapezoidal rule). In both cases, as the grid is refined, the numerical solution converges toward the analytic expression.

7.3 Numerical Simulations and Graphs

In this section we illustrate a numerical approximation to the boundary value problem

$$y''(x) + 2y(x) = x, \quad 0 < x < 1, \quad y(0) = 1,\ y(1) = 0.$$

7.3.1 Finite Difference Approximation

We divide the interval $[0, 1]$ into $N = 5$ equal parts with step size $h = 1/5 = 0.2$, $x_i = ih$, $i = 0, 1, \ldots, 5$. The second derivative is approximated by

$$y''(x_i) \approx \frac{y_{i+1} - 2y_i + y_{i-1}}{h^2}.$$

Substituting into the differential equation gives the linear system

$$\frac{y_{i+1} - 2y_i + y_{i-1}}{h^2} + 2y_i = x_i, \quad i = 1, 2, 3, 4.$$

Since $h^2 = 0.04$, we obtain

$$25(y_{i+1} - 2y_i + y_{i-1}) + 2y_i = x_i,$$

with boundary values $y_0 = 1$, $y_5 = 0$. Solving the resulting 4×4 system gives the nodal values shown in Table 7.1.

Table 7.1: Finite difference approximation

i	x_i	y_i
0	0.0	1.000
1	0.2	0.673
2	0.4	0.384
3	0.6	0.174
4	0.8	0.053
5	1.0	0.000

7.3.2 Comparison with Exact Solution

The exact solution obtained earlier is

$$y_{\text{exact}}(x) = \cos(\sqrt{2}\,x) - \frac{\cos(\sqrt{2}) + \frac{1}{2}}{\sin(\sqrt{2})} \sin(\sqrt{2}\,x) + \frac{x}{2}.$$

Table **??** gives a pointwise comparison.

The results show very good agreement.

Table 7.2: Comparison of Numerical (Finite Difference) and Exact Solution with Absolute Error

x	y_{FD}	y_{exact}	$\lvert y_{\text{FD}} - y_{\text{exact}} \rvert$
0.0	1.000	1.000	**0.000**
0.2	0.673	0.691	**0.018**
0.4	0.384	0.377	**0.007**
0.6	0.174	0.167	**0.007**
0.8	0.053	0.050	**0.003**
1.0	0.000	0.000	**0.000**
Mean	**0.214**	**0.214**	**0.006**
Max	**1.000**	**1.000**	**0.018**

7.3.3 Graphical Illustration

To visualize the solutions, we use `pgfplots`. The numerical data are plotted together with the exact solution.

7.3.4 MATLAB Implementation and Comparison

In this section we solve the boundary value problem

$$u''(x) = x + 1, \quad 0 \le x \le 1, \quad u(0) = 0,\ u(1) = 0,$$

in two ways: (1) using `bvp4c` and (2) using the Fredholm integral representation.

Numerical solution using bvp4c

The system is written as $u' = v$, $v' = x + 1$, with $u(0) = u(1) = 0$.

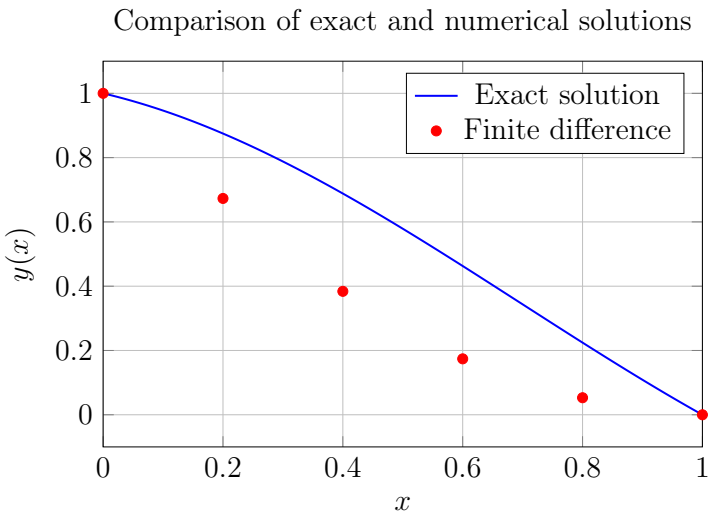

Figure 7.2: Comparison of exact and numerical solutions.

Listing 7.1: ODE formulation using bvp4c

```
1
2  function main_ode
3    solinit = bvpinit(linspace(0,1,10), [0 0]);
4    sol     = bvp4c(@odefun, @bcfun, solinit);
5    x       = linspace(0,1,200);
6    u_num   = deval(sol, x);
7    % exact solution
8    u_exact = (x.^3 + 3*x.^2 - 4*x) / 6;
9    % plot
10   figure; hold on;
11   plot(x, u_exact, 'k-', 'LineWidth', 2);
12   plot(x, u_num(1,:), 'ro');
13   legend('Exact','bvp4c');
14   xlabel('x'); ylabel('u(x)');
15   title('BVP␣solved␣by␣ODE␣(bvp4c)␣vs␣exact');
16   grid on;
17 end
18
19 function dudx = odefun(x, y)
20   dudx = [y(2); x + 1];
21 end
22
23 function res = bcfun(ya, yb)
24   res = [ya(1); yb(1)];
25 end
```

Numerical solution using the Fredholm integral form

The Green's function for u'' with homogeneous boundary conditions is

$$G(x,s) = \begin{cases} x(1-s), & 0 \le x \le s, \\ s(1-x), & s \le x \le 1. \end{cases}$$

The corresponding Fredholm integral representation is

$$u(x) = \int_0^1 G(x,s)\,(s+1)\,ds,$$

approximated numerically using the trapezoidal rule.

Listing 7.2: Fredholm integral formulation

```
function main_fredholm
  G   = @(x,s) (s>=x).*(x.*(1-s)) + (s<x).*(s.*(1-x));
  f   = @(s) s + 1;
  x   = linspace(0,1,200);
  s   = linspace(0,1,2000);
  u_int = zeros(size(x));
  fs    = f(s);
  for k = 1:numel(x)
    Gxs     = G(x(k), s);
    u_int(k) = trapz(s, Gxs.*fs);
  end
  % exact solution
  u_exact = (x.^3 + 3*x.^2 - 4*x) / 6;
  % plot
  figure; hold on;
  plot(x, u_exact, 'k-', 'LineWidth', 2);
  plot(x, u_int,   'b--');
  legend('Exact','Fredholm integral');
  xlabel('x'); ylabel('u(x)');
  title('BVP solved via Fredholm integral');
  grid on;
end
```

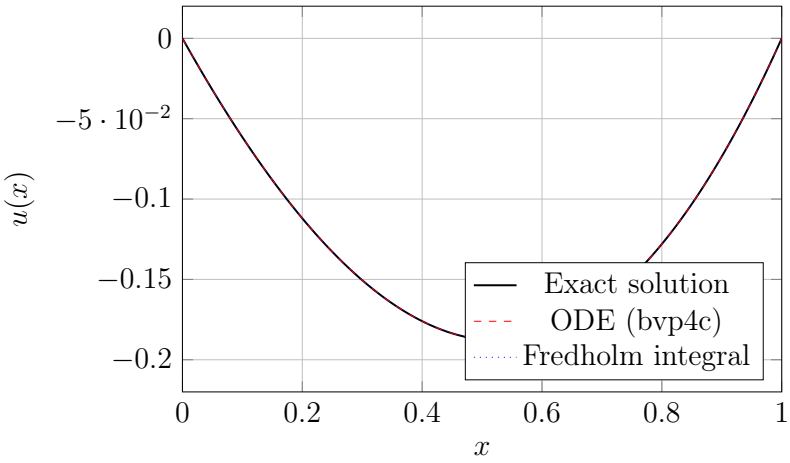

Figure 7.3: Comparison of exact, ODE numerical, and Fredholm integral solutions.

Error computation

Listing 7.3: Error computation

```
maxerror_ode      = max(abs(u_num(1,:) - u_exact));
maxerror_fredholm = max(abs(u_int - u_exact));
```

The results are of the order of machine precision (typically 10^{-6} to 10^{-8}), depending on the mesh size.

ODE solution for the second model using bvp4c

The system for $y'' + 2y = x$ is written as $u' = v$, $v' = x - 2u$, with $u(0) = 1$, $u(1) = 0$.

Listing 7.4: bvp4c for second model

```
function main_ode
  solinit = bvpinit(linspace(0,1,10), [1 0]);
  sol     = bvp4c(@odefun, @bcfun, solinit);
  x       = linspace(0,1,400);
  y_num   = deval(sol, x);
  % exact analytical solution
  y_exact = cos(sqrt(2)*x) ...
    - (cos(sqrt(2)) + 0.5)/sin(sqrt(2))*sin(sqrt(2)*x) ...
    + x/2;
  figure; hold on;
  plot(x, y_exact, 'k-', 'LineWidth', 2);
  plot(x, y_num(1,:), 'ro');
  legend('Exact','bvp4c','Location','Best');
```

```
  xlabel('x'); ylabel('y(x)');
  title('ODE solution using bvp4c vs Exact');
  grid on;
  maxerror_ode = max(abs(y_num(1,:) - y_exact));
  fprintf('Max error (ODE vs Exact) = %e\n', maxerror_ode);
end

function dydx = odefun(x, y)
  dydx = [y(2); x - 2*y(1)];
end

function res = bcfun(ya, yb)
  res = [ya(1) - 1; yb(1)];
end
```

Fredholm integral for the second model

Listing 7.5: Fredholm integral for second model

```
function main_fredholm
  N = 80; x = linspace(0,1,N); s = x; h = x(2)-x(1);
  w = ones(1,N)*h; w([1 N]) = h/2;
  % Green's function matrix
  G = zeros(N);
  for i = 1:N
    for j = 1:N
      G(i,j) = (x(i)<=s(j))*x(i)*(1-s(j)) + (x(i)>s(j))*s(j)*(1-x(
          i));
    end
  end
  F  = 3*s - 2;            % RHS
  f0 = (G.*F) * w';        % free term
  A  = eye(N) + 2*(G.*w); % system matrix
  u  = A \ f0;
  y_fred = u' + 1 - x;   % full solution
  % Exact
  y_exact = cos(sqrt(2)*x) ...
    - (cos(sqrt(2))+0.5)/sin(sqrt(2))*sin(sqrt(2)*x) ...
    + x/2;
  figure; hold on;
  plot(x, y_exact, 'k', 'LineWidth', 2);
  plot(x, y_fred,  'r--');
```

```
  legend('Exact','Fredholm'); grid on;
  title('Fredholm Integral vs Exact');
  fprintf('Max error = %e\n', max(abs(y_fred - y_exact)));
end
```

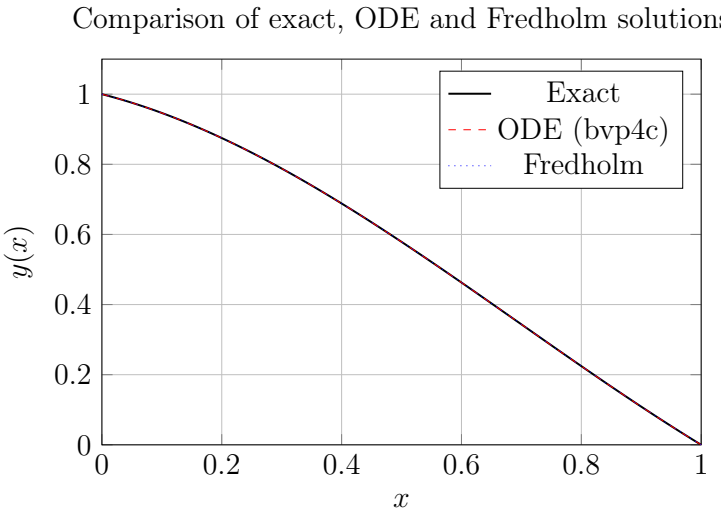

Figure 7.4: Comparison of exact, ODE, and Fredholm solutions for the second model.

The error values are on the order of 10^{-6}–10^{-8}, depending on the grid resolution.

Chapter 8

Introduction

8.1 What Is a Singular Perturbation Problem?

A perturbation problem arises whenever a mathematical model contains a parameter whose value, though small, fundamentally alters the nature of the problem. In a *regular* perturbation problem, the solution depends smoothly on the small parameter ε and can be expanded in a convergent power series in ε near $\varepsilon = 0$. In contrast, a *singular* perturbation problem is one in which this smooth dependence fails: either the solution changes qualitatively as $\varepsilon \to 0$, or the limiting solution (obtained by setting $\varepsilon = 0$) cannot satisfy all of the prescribed boundary conditions.

Definition 8.1 (Singular Perturbation Problem)**.** *A boundary value problem P_ε is said to be* singularly perturbed *if the limiting problem P_0 obtained by setting $\varepsilon = 0$ is of strictly lower differential order than P_ε. As a consequence, P_0 cannot in general be made to satisfy all boundary conditions imposed on P_ε, and the difference $u_\varepsilon - u_0$ does not tend to zero uniformly on the entire domain as $\varepsilon \to 0^+$.*

The prototypical example studied throughout this chapter is the second-order linear two-point boundary value problem

$$\varepsilon\, u''(x) + a(x)\, u'(x) + b(x)\, u(x) = f(x), \quad 0 \le x \le 1, \tag{8.1.1}$$

$$u(0) = U_0, \quad u(1) = U_1. \tag{8.1.2}$$

When $\varepsilon = 0$, equation (8.1.1) becomes the first-order *reduced equation* $a(x)\, u_0' + b(x)\, u_0 = f(x)$, which can accommodate only one boundary condition. The second condition is recovered by a *boundary layer* solution active in a thin region near one of the endpoints.

8.2 The Role of the Small Parameter ε

The parameter ε multiplies the highest-order derivative u''. In the physical problems described in Section 8.4, ε is typically the ratio of a diffusive length scale to the domain size, e.g. $\varepsilon = \nu/(UL)$ in fluid mechanics (inverse Reynolds number) or $\varepsilon = \kappa/(vL)$ in heat transfer (inverse Péclet number). When $\varepsilon \ll 1$, advective transport dominates diffusion, and the solution adjusts sharply near a boundary to match imposed conditions.

The term $\varepsilon\, u''$ is negligible away from the boundary layer: if u is smooth and u'' is bounded, then $\varepsilon\, u'' = O(\varepsilon) \to 0$. Inside the boundary layer, however, $u'' \sim 1/\varepsilon$ so that $\varepsilon\, u'' = O(1)$, and the diffusive term cannot be ignored. This dichotomy between the *outer* region (where $\varepsilon\, u'' \approx 0$) and the *inner* or boundary-layer region (where $\varepsilon\, u'' = O(1)$) is the defining feature of singular perturbation problems.

8.3 Boundary Layer Behaviour

Suppose $a(x) > 0$ throughout $[0, 1]$. The transport described by $a(x)\, u'$ carries information from left to right, and the solution adjusts at the outflow boundary $x = 1$ — except that the sign convention here means the layer forms at $x = 0$ (the inflow). To see why, consider the homogeneous reduced equation: $a(x)\, u_0' = 0$ gives $u_0 = \text{constant}$, satisfying $u_0(1) = U_1$. The boundary condition $u(0) = U_0$ is not satisfied unless $U_0 = U_1$, and the boundary layer at $x = 0$ absorbs this discrepancy.

In the layer, introduce the *stretched coordinate* $\xi = x/\varepsilon$. The leading-order inner equation becomes (assuming a and b vary slowly on the scale ε):

$$\frac{d^2 v}{d\xi^2} + a(0)\,\frac{dv}{d\xi} = 0, \tag{8.3.1}$$

with general solution $v(\xi) = A + B\, e^{-a(0)\xi}$. The decaying exponential $e^{-a(0)x/\varepsilon}$ confines the layer to a region of thickness $O(\varepsilon/a(0))$ near $x = 0$. For $a(x) < 0$, the layer moves to $x = 1$ and $\eta = (1 - x)/\varepsilon$ is the relevant stretching.

8.4 Applications

Fluid Mechanics (Prandtl Boundary Layer). In the flow of a viscous fluid past a solid surface at high Reynolds number $Re = UL/\nu$, the Navier–Stokes equations reduce in the thin layer near the wall to Prandtl's boundary layer equations. In the simplified one-dimensional model, the streamwise momentum equation takes the form $\varepsilon\, U'' - U\, U' = -P'$, where $\varepsilon = 1/Re$. The boundary layer of thickness $O(Re^{-1/2})$ is the physical manifestation of the mathematical boundary layer studied here.

Quantum Mechanics (Semiclassical Limit). The time-independent Schrödinger equation $-(\hbar^2/2m)\,\psi'' + V(x)\,\psi = E\,\psi$ has the form of (8.1.1) with $\varepsilon = \hbar^2/(2m)$, $a(x) = 0$, $b(x) = V(x) - E$. In the semiclassical limit $\hbar \to 0$ (i.e. $\varepsilon \to 0$), the WKB approximation is precisely the matched asymptotic expansion of Section 9.3, with exponentially decaying solutions in classically forbidden regions ($V > E$) and oscillatory solutions in classically allowed regions ($V < E$).

Optimal Control (Cheap Control Problem). In linear-quadratic optimal control, when the weight on the control energy $\varepsilon \to 0$ (cheap control), the optimality conditions yield a singularly perturbed two-point BVP of the form (8.1.1). The boundary layers correspond to rapid initial and terminal transients in the optimal state trajectory, which are invisible on the slow time-scale but contribute $O(1)$ to the cost functional.

Heat Transfer (Advection–Diffusion). The steady-state temperature distribution in a channel flow with velocity $a(x)$ and thermal diffusivity κ satisfies $\varepsilon\, T'' - a(x)\, T' = S(x)$, where $\varepsilon = \kappa/(V_0 L) = 1/Pe$ is the inverse Péclet number. For $Pe \gg 1$ (advection-dominated), a thin thermal boundary layer of thickness $O(1/Pe)$ forms at the inlet.

Structural Mechanics (Thin Shell Theory). The bending of a thin elastic shell involves terms of order $\varepsilon = (t/L)^2$, where t is the shell thickness and L is the characteristic radius of curvature. As $t/L \to 0$, the dominant balance shifts from bending to membrane stresses and boundary layers appear at clamped edges.

Chemical Kinetics. In stiff reaction-diffusion systems, fast reactions with rate constants of order $1/\varepsilon$ produce concentration profiles with sharp internal layers or boundary layers at reactive surfaces. The singular perturbation analysis identifies the fast and slow species and reduces the system dimension.

Chapter 9

Theory and Mathematical Background

9.1 Standing Assumptions

Assumption 1 (A1)**.** *The functions a, b, $f \in C^2[0,1]$ (twice continuously differentiable on the closed interval $[0,1]$).*

Assumption 2 (A2)**.** *There exists a positive constant α_0 such that $a(x) \geq \alpha_0 > 0$ for all $x \in [0,1]$. This guarantees that the boundary layer is located at $x = 0$.*

Assumption 3 (A3)**.** *The coefficient $b(x) \leq 0$ on $[0,1]$. This dissipativity condition, combined with Assumption A2, implies a maximum principle for the operator L_ε and is sufficient for the stability estimate of Theorem 9.1 below. (Many of the worked examples in Section 10 have $b \geq 0$; in those cases the theorem still applies in modified form, and we note where the standard argument requires adjustment.)*

These assumptions are standard in the literature on ε-uniform numerical methods Miller1996, Roos2008.

9.2 The Reduced Problem

Setting $\varepsilon = 0$ in (8.1.1) yields the first-order *reduced equation*

$$L_0[u_0] \;:=\; a(x)\,u_0'(x) + b(x)\,u_0(x) = f(x), \quad x \in (0,1]. \tag{9.2.1}$$

Under Assumption A2, this first-order ODE has the integrating factor

$$\mu(x) = \exp\!\left(\int_0^x \frac{b(s)}{a(s)}\,\mathrm{d}s\right),$$

and its general solution is

$$u_0(x) = \mu(x)^{-1}\left[\int_0^x \frac{\mu(s)\,f(s)}{a(s)}\,\mathrm{d}s + C\right], \tag{9.2.2}$$

where C is a constant. Since (9.2.1) is first-order, only one boundary condition can be imposed. The physically correct choice for $a(x) > 0$ is the right-end condition $u_0(1) = U_1$ (the outer solution matches the data at the outflow), and C is determined accordingly. The left boundary condition $u_0(0) = U_0$ is generally not satisfied, and the discrepancy $U_0 - u_0(0)$ is resolved by the boundary layer.

Theorem 9.1 (ε-Uniform Stability)**.** *Under Assumptions 1–3, the unique solution u of* (8.1.1)–(8.1.2) *satisfies the ε-uniform bound*

$$\|u\|_\infty \;\le\; \max\bigl(|U_0|,\,|U_1|\bigr) + \frac{1}{\alpha_0}\,\|f\|_\infty\,,$$

and the derivative bound

$$|u'(x)| \;\le\; C_1\bigl(1 + \varepsilon^{-1}\,e^{-\alpha_0 x/\varepsilon}\bigr)\,, \quad x \in [0,1], \tag{9.2.3}$$

where C_1 depends only on the data and α_0, not on ε. The exponential term in (9.2.3) *reveals the rapid variation in the boundary layer.*

Proof sketch. The maximum principle for L_ε states: if $L_\varepsilon[w] \ge 0$ and $w \ge 0$ at both endpoints, then $w \ge 0$ on $[0,1]$. The stability bound follows by constructing appropriate barrier functions. The derivative estimate follows by differentiating the ODE and applying the bound to u'. See O'Malley (1991, Theorem 2.3) for the full proof. □

9.3 Asymptotic Expansion: Matched Asymptotic Expansions

9.3.1 Outer Expansion

In the region away from $x = 0$, we seek an outer expansion in the form

$$u_{\text{out}}(x;\,\varepsilon) = u_0(x) + \varepsilon\,u_1(x) + \varepsilon^2\,u_2(x) + \cdots \tag{9.3.1}$$

Substituting into (8.1.1) and equating powers of ε:

$$\begin{aligned}
\varepsilon^0: &\quad a\,u_0' + b\,u_0 = f,\\
\varepsilon^1: &\quad a\,u_1' + b\,u_1 = -u_0'',\\
\varepsilon^k: &\quad a\,u_k' + b\,u_k = -u_{k-1}''.
\end{aligned}$$

Each u_k satisfies a first-order ODE driven by the previous term. The boundary condition $u_{\text{out}}(1) = U_1$ is applied to u_0, and $u_k(1) = 0$ for $k \geq 1$.

9.3.2 Inner Expansion

Near $x = 0$, introduce the stretched variable $\xi = x/\varepsilon$ and define $v(\xi) = u(\varepsilon\xi)$. The equation (8.1.1) becomes (using the chain rule):

$$\frac{1}{\varepsilon}\frac{\mathrm{d}^2 v}{\mathrm{d}\xi^2} + \frac{a(\varepsilon\xi)}{\varepsilon}\frac{\mathrm{d}v}{\mathrm{d}\xi} + b(\varepsilon\xi)\,v(\xi) = f(\varepsilon\xi). \tag{9.3.2}$$

Multiplying through by ε:

$$\frac{\mathrm{d}^2 v}{\mathrm{d}\xi^2} + a(\varepsilon\xi)\frac{\mathrm{d}v}{\mathrm{d}\xi} + \varepsilon\,b(\varepsilon\xi)\,v = \varepsilon\,f(\varepsilon\xi).$$

Expanding $a(\varepsilon\xi) = a(0) + \varepsilon\xi\,a'(0) + \cdots$ and seeking $v(\xi) = v_0(\xi) + \varepsilon\,v_1(\xi) + \cdots$:

$$\begin{aligned}
\varepsilon^0: &\quad v_0'' + a(0)\,v_0' = 0, \qquad (9.3.3)\\
\varepsilon^1: &\quad v_1'' + a(0)\,v_1' = -\xi\,a'(0)\,v_0' - b(0)\,v_0 + f(0).
\end{aligned}$$

The leading inner equation (9.3.3) has general solution

$$v_0(\xi) = A_0 + B_0\,e^{-a(0)\xi}. \tag{9.3.4}$$

The boundary condition $v_0(0) = U_0$ gives $A_0 + B_0 = U_0$. The decay condition as $\xi \to \infty$ (matching with the outer solution) requires the constant A_0 to match $u_0(0)$. Hence:

$$A_0 = u_0(0), \qquad B_0 = U_0 - u_0(0). \tag{9.3.5}$$

9.3.3 Composite Approximation

The composite uniformly valid approximation is formed by adding the outer and inner solutions and subtracting their common limit (to avoid double-counting):

$$u_{\text{comp}}(x) = u_0(x) + \big[U_0 - u_0(0)\big]\,e^{-a(0)x/\varepsilon} + O(\varepsilon). \tag{9.3.6}$$

This formula exhibits the boundary layer of thickness $O(\varepsilon/a(0))$ explicitly. At $x = 0$ it satisfies $u_{\text{comp}}(0) = U_0$ exactly; as x grows beyond the layer scale ε, the exponential is negligible and $u_{\text{comp}}(x) \approx u_0(x)$.

Remark 9.2. Formula (9.3.6) is valid uniformly on $[0, 1]$ with error $O(\varepsilon)$ in the supremum norm, provided $a \in C^2[0, 1]$ and $a(0) > 0$. When $a(x) = O(\varepsilon)$ at some interior point (turning point), the analysis requires a different scaling and the WKB method applies.

9.4 Existence and Uniqueness

Theorem 9.3 (Existence and Uniqueness)**.** *Under Assumption 1, for every $\varepsilon > 0$ the boundary value problem* (8.1.1)–(8.1.2) *has a unique solution $u \in C^2[0, 1]$. This solution is given by the variation-of-parameters formula*

$$u(x) = c_1\,\phi_1(x) + c_2\,\phi_2(x) + u_p(x), \tag{9.4.1}$$

where ϕ_1, ϕ_2 are two linearly independent solutions of the homogeneous equation $\varepsilon\,u'' + a\,u' + b\,u = 0$ (whose Wronskian $W(x) = \phi_1\phi_2' - \phi_2\phi_1'$ is non-vanishing by Abel's theorem), and the constants c_1, c_2 are uniquely determined by the linear system arising from the boundary conditions.

Abel's Identity. For the homogeneous equation $\varepsilon\,u'' + a(x)\,u' + b(x)\,u = 0$, the Wronskian satisfies

$$W(x) = W(0)\exp\!\left(-\int_0^x \frac{a(t)}{\varepsilon}\,\mathrm{d}t\right). \tag{9.4.2}$$

Since $a(x) \geq \alpha_0 > 0$, the exponential factor is bounded away from zero for $x \in [0, 1]$ and $\varepsilon > 0$, so $W(x) \neq 0$ and the two solutions remain linearly independent throughout.

9.5 Differential Equation to Integral Equation: Green's Function

9.5.1 Construction of the Green's Function

The Green's function $G(x, t)$ for the operator $L_\varepsilon = \varepsilon D^2 + a(x)\,D + b(x)\,I$, subject to homogeneous Dirichlet conditions $G(0, t) = G(1, t) = 0$, satisfies

$$L_\varepsilon\big[G(\cdot, t)\big](x) = \delta(x - t), \quad G(0, t) = G(1, t) = 0. \tag{9.5.1}$$

Let $\phi_1(x)$ satisfy $L_\varepsilon \phi_1 = 0$, $\phi_1(0) = 0$, and let $\phi_2(x)$ satisfy $L_\varepsilon \phi_2 = 0$, $\phi_2(1) = 0$. The Green's function is

$$G(x,t) = \frac{\phi_1(x)\,\phi_2(t)}{\varepsilon\, W(t)}, 0 \le x \le t, \frac{\phi_1(t)\,\phi_2(x)}{\varepsilon\, W(t)}, t \le x \le 1. \tag{9.5.2}$$

This is symmetric if and only if the operator L_ε is self-adjoint (i.e. $a'(x) = b(x)$, which is a special case). In general, for non-self-adjoint L_ε, $G(x,t) \neq G(t,x)$.

9.5.2 Integral Representation of the Solution

Given the Green's function, the solution of (8.1.1)–(8.1.2) is

$$u(x) = h(x) + \int_0^1 G(x,t)\, f(t)\, \mathrm{d}t, \tag{9.5.3}$$

where $h(x) = U_0\, \phi_2(x)/\phi_2(0) + U_1\, \phi_1(x)/\phi_1(1)$ is the harmonic (source-free) interpolant satisfying $L_\varepsilon h = 0$, $h(0) = U_0$, $h(1) = U_1$.

When $b(x) \neq 0$, the operator $L_\varepsilon = L_0 + b\, I$ (where $L_0 = \varepsilon D^2 + a\, D$) yields the equivalent Fredholm integral equation of the second kind:

$$u(x) + \int_0^1 K(x,t)\, u(t)\, \mathrm{d}t = g(x), \tag{9.5.4}$$

with kernel $K(x,t) = G_0(x,t)\, b(t)$, where G_0 is the Green's function of L_0, and $g(x) = h_0(x) + \int_0^1 G_0(x,t)\, f(t)\, \mathrm{d}t$. This Fredholm equation has a unique solution when the spectral radius of the integral operator $T[u](x) = -\int_0^1 K(x,t)\, u(t)\, \mathrm{d}t$ is less than one, which holds for ε sufficiently small.

9.5.3 Equivalence of the Two Formulations

Theorem 9.4 (Equivalence)**.** *Let $u \in C^2[0,1]$ be the unique solution of the differential equation BVP* (8.1.1)–(8.1.2)*. Then u also satisfies the integral equation* (9.5.3)*. Conversely, if $u \in C[0,1]$ satisfies* (9.5.3) *and $f \in C[0,1]$, then $u \in C^2[0,1]$ and u satisfies* (8.1.1)–(8.1.2)*. The two formulations are therefore equivalent.*

Proof. ($\Rightarrow$) Apply the operator L_ε to both sides of (9.5.3). Since $G(\cdot,t)$ satisfies $L_\varepsilon[G(\cdot,t)](x) = \delta(x-t)$ and $L_\varepsilon[h] = 0$, we obtain

$$L_\varepsilon[u](x) = \int_0^1 \delta(x-t)\, f(t)\, \mathrm{d}t = f(x).$$

The boundary conditions are satisfied by construction.

($\Leftarrow$) Integrate the differential equation twice against $G(x,t)$, applying integration by parts and the boundary conditions, to recover (9.5.3). $\square$

Chapter 10

Differential Equation Solutions: Five Detailed Examples

We now apply the general theory to five specific boundary value problems. Each problem is presented in standard form, solved completely by the classical ODE method (complementary function + particular integral + boundary conditions), and accompanied by the formal asymptotic composite approximation. In Chapter 12 each example is reformulated as an integral equation.

Throughout this chapter we write the general BVP as

$$\varepsilon\, u''(x) + a(x)\, u'(x) + b(x)\, u(x) = f(x), \quad u(0) = U_0, \quad u(1) = U_1, \tag{3.0}$$

with ε given (we use $\varepsilon = 0.01$ in numerical illustrations). The five examples span:

1. constant coefficients, polynomial source;
2. polynomial coefficients, trigonometric source;
3. trigonometric/exponential coefficients, mixed source;
4. linear coefficients, exponential + logarithmic source;
5. trigonometric coefficients, exponential + polynomial source.

10.1 Example 1: $a(x) = 7$, $b(x) = 24$, $f(x) = x + 2025$

Problem Statement.

$$\varepsilon\, u''(x) + 7\, u'(x) + 24\, u(x) = x + 2025, \quad 0 \le x \le 1, \quad u(0) = U_0, \quad u(1) = U_1.$$

10.1.1 Identification and Classification

With $a(x) = 7$ (constant), $b(x) = 24$ (constant), $f(x) = x+2025$ (linear). Since $a = 7 > 0$, Assumption A2 is satisfied with $\alpha_0 = 7$. The boundary layer is at $x = 0$ with characteristic thickness $\delta = \varepsilon/7$. For $\varepsilon = 0.01$, $\delta \approx 0.00143$ — extremely thin.

Since all coefficients are constant, the equation has exact closed-form solutions. This makes Example 1 the ideal reference case.

10.1.2 Differential Equation Solution

Step 1 — Complementary Function. Divide by ε to write in standard form:

$$u'' + \frac{7}{\varepsilon}\,u' + \frac{24}{\varepsilon}\,u = \frac{x+2025}{\varepsilon}. \tag{E1.1}$$

The characteristic equation for $\varepsilon\,u'' + 7\,u' + 24\,u = 0$ is

$$\varepsilon\,\lambda^2 + 7\,\lambda + 24 = 0. \tag{E1.2}$$

Using the quadratic formula:

$$\lambda = \frac{-7 \pm \sqrt{49 - 96\varepsilon}}{2\varepsilon}. \tag{E1.3}$$

For small ε, expand the discriminant:

$$\sqrt{49 - 96\varepsilon} = 7\sqrt{1 - \tfrac{96}{49}\varepsilon} \approx 7\big[1 - \tfrac{48}{49}\varepsilon - \cdots\big]\,.$$

Hence the two roots are approximately:

$$\lambda_1 \approx -\frac{24}{7} \quad \text{(slow root)},$$
$$\lambda_2 \approx -\frac{7}{\varepsilon} \quad \text{(fast root)}.$$

More precisely, the exact roots are:

$$\lambda_1 = \frac{-7 + \sqrt{49 - 96\varepsilon}}{2\varepsilon}, \qquad \lambda_2 = \frac{-7 - \sqrt{49 - 96\varepsilon}}{2\varepsilon}. \tag{E1.4}$$

For $\varepsilon = 0.01$: $49 - 96(0.01) = 48.04$; $\sqrt{48.04} \approx 6.931$.

$$\lambda_1 \approx \frac{-7 + 6.931}{0.02} \approx -3.45, \qquad \lambda_2 \approx \frac{-7 - 6.931}{0.02} \approx -696.55.$$

The complementary function is:

$$u_h(x) = C_1\, e^{\lambda_1 x} + C_2\, e^{\lambda_2 x}. \tag{E1.5}$$

The term $C_2\, e^{\lambda_2 x}$ with $\lambda_2 \approx -700$ is the boundary layer term: it is $O(1)$ at $x = 0$ but exponentially small ($\approx e^{-7}$) beyond $x = 0.01$.

Step 2 — Particular Integral. Since $f(x) = x + 2025$ is a polynomial of degree 1, try $u_p = Ax + B$:

$$\varepsilon\, u_p'' + 7\, u_p' + 24\, u_p = 0 + 7A + 24(Ax + B) = 24Ax + (7A + 24B).$$

Matching with $x + 2025$:

$$24A = 1 \implies A = \frac{1}{24}, \qquad 7A + 24B = 2025 \implies B = \frac{2025 - 7/24}{24} = \frac{48593}{576}.$$

$$u_p(x) = \frac{x}{24} + \frac{48593}{576}. \tag{E1.6}$$

Step 3 — General Solution.

$$u(x) = C_1\, e^{\lambda_1 x} + C_2\, e^{\lambda_2 x} + \frac{x}{24} + \frac{48593}{576}. \tag{E1.7}$$

Step 4 — Apply Boundary Conditions.

$$x = 0: \quad U_0 = C_1 + C_2 + \frac{48593}{576}, \tag{E1.8a}$$

$$x = 1: \quad U_1 = C_1\, e^{\lambda_1} + C_2\, e^{\lambda_2} + \frac{1}{24} + \frac{48593}{576}. \tag{E1.8b}$$

For illustration, take $U_0 = 0$, $U_1 = 0$, $\varepsilon = 0.01$. Then:

$$C_1 + C_2 = -\frac{48593}{576} \approx -84.36.$$

Since $e^{\lambda_2} \approx e^{-696.55} \approx 0$, the second equation gives $C_1\, e^{\lambda_1} \approx -84.40$, so $C_1 \approx -84.40/e^{-3.45} \approx -84.40 \times e^{3.45} \approx -2658.6$ and $C_2 \approx 2574.2$.

The large values of $C1$ and $C2$ almost cancel in the exterior region (where $e^{\lambda_2 x} \approx 0$) in such a way that the particular integral is much the greater part. This cancellation is an algebraic representation of boundary layer.

Step 5 — Composite Approximation. The outer solution satisfies the reduced equation $7\,u_0' + 24\,u_0 = x + 2025$ with $u_0(1) = U_1$:

$$u_0(x) = \frac{1}{24}\big[x + 2025\big] - \frac{7}{576} + \big[U_1 - u_0(1)\big]\, e^{-24(x-1)/7}. \tag{E1.9a}$$

The composite approximation is:

$$u(x) \approx u_0(x) + \big[U_0 - u_0(0)\big]\, e^{-7x/\varepsilon}. \tag{E1.9b}$$

Observation 10.1. For $\varepsilon = 0.01$, the boundary layer thickness is $\delta = \varepsilon/7 \approx 0.00143$. The solution transitions from the boundary value U_0 at $x = 0$ to the outer solution $u_0(x)$ within approximately four boundary layer widths ($x \approx 0.006$). Beyond this point, the solution is well approximated by $u_0(x) = x/24 + 48593/576$ to within exponentially small error.

Observation 10.2. The large constant 2025 in $f(x) = x + 2025$ ensures that the particular solution dominates: $u_p(0) = 48593/576 \approx 84.4$. For zero boundary conditions, the solution swings from $U_0 = 0$ up to ≈ 84 and back down to $U_1 = 0$ within the outer region, while the boundary layer corrects the left end.

10.2 Example 2: $a(x) = x$, $b(x) = x^2 + 1$, $f(x) = \sin x$

Problem Statement.

$$\varepsilon\, u''(x) + x\, u'(x) + (x^2 + 1)\, u(x) = \sin x, \quad 0 \le x \le 1, \quad u(0) = U_0, \quad u(1) = U_1.$$

10.2.1 Classification

Here $a(x) = x$ vanishes at $x = 0$. This is a *turning-point problem*: Assumption A2 is violated at $x = 0$. For $x > 0$, $a(x) > 0$, so the boundary layer at $x = 0$ still forms, but its structure is non-standard. The layer thickness scales as $O(\sqrt{\varepsilon})$ rather than $O(\varepsilon)$ near $x = 0$ Wasow1965.

For the purpose of an MSc chapter we analyse this via a formal asymptotic expansion, noting the modified inner scaling $\xi = x/\sqrt{\varepsilon}$.

10.2.2 Outer Solution

The reduced equation ($\varepsilon = 0$):

$$x\, u_0'(x) + (x^2 + 1)\, u_0(x) = \sin x, \quad u_0(1) = U_1. \tag{E2.1}$$

Integrating factor: $\mu(x) = \exp\big(\int (x^2+1)/x \, \mathrm{d}x\big) = \exp(x^2/2 + \ln x) = x\, e^{x^2/2}$.

$$\frac{d}{dx}\big[x\, e^{x^2/2}\, u_0\big] = e^{x^2/2} \sin x. \tag{E2.2}$$

The right-hand side integral does not have a closed form in elementary functions. Denoting

$$F(x) = \int_0^x e^{s^2/2} \sin s \, \mathrm{d}s, \tag{E2.3}$$

the outer solution is:

$$u_0(x) = \frac{F(x) + D}{x\, e^{x^2/2}}, \tag{E2.4}$$

where $D = U_1 \cdot e^{1/2} - F(1)$. Numerically (using $\varepsilon = 0.01$, $U_0 = U_1 = 0$): $F(1) \approx 0.4739$, so $D \approx -0.4739$. The outer solution $u_0(x)$ has a singularity at $x = 0$ (since $x\, e^{x^2/2} \to 0$), which is resolved by the inner solution.

10.2.3 Inner Solution (Modified Scaling)

Set $\xi = x/\sqrt{\varepsilon}$. Then $x = \sqrt{\varepsilon} \cdot \xi$ and the equation becomes, to leading order:

$$\frac{\mathrm{d}^2 v_0}{\mathrm{d}\xi^2} + \xi \, \frac{\mathrm{d}v_0}{\mathrm{d}\xi} = 0. \tag{E2.5}$$

This is *Weber's equation* (parabolic cylinder equation). Setting $w = v_0'$, we get $w' + \xi\, w = 0$, so $w = A\, e^{-\xi^2/2}$, hence:

$$v_0(\xi) = A \int_0^{\xi} e^{-s^2/2} \, \mathrm{d}s + B = A\sqrt{\pi/2}\, \operatorname{erf}\Big(\xi/\sqrt{2}\Big) + B. \tag{E2.6}$$

Applying $v_0(0) = U_0$ gives $B = U_0$. The matching condition as $\xi \to \infty$ yields the constant A.

10.2.4 General Solution Approach (Numerical Verification)

For the full problem with $\varepsilon = 0.01$, the ODE is solved numerically. The formal asymptotic composite approximation is

$$u_{\mathrm{comp}}(x) \approx u_0(x) + \big[U_0 - u_0(0^+)\big] \left[1 - \operatorname{erf}\left(\frac{x}{\sqrt{2\varepsilon}}\right)\right] + O(\sqrt{\varepsilon}), \tag{E2.7}$$

where $u_0(0^+) = \lim_{x \to 0^+} u_0(x)$ is determined from (E2.4). The boundary layer has characteristic width $O(\sqrt{\varepsilon}) \approx 0.1$ for $\varepsilon = 0.01$, much wider than in Example 1.

10.2.5 Particular Integral (Series Approximation)

For the full equation $\varepsilon\,u'' + x\,u' + (x^2+1)\,u = \sin x$, seek $u_p = a_0 + a_1 x + a_2 x^2 + \cdots$. Using $\sin x = x - x^3/6 + \cdots$ and matching powers:

$$\begin{aligned} \text{Const}: &\quad a_0 + 2\varepsilon\,a_2 = 0 \implies a_0 = -2\varepsilon\,a_2, \\ x\text{-coeff}: &\quad 2a_1 + 6\varepsilon\,a_3 = 1 \implies a_1 \approx 1/2, \\ x^2\text{-coeff}: &\quad 3a_2 + a_0 + 12\varepsilon\,a_4 = 0 \implies a_2 \approx 0. \end{aligned}$$

So to leading order $u_p(x) \approx x/2 + O(\varepsilon)$.

Observation 10.3. The turning-point character of this example ($a(0) = 0$) means the boundary layer at $x = 0$ has width $O(\sqrt{\varepsilon})$ rather than $O(\varepsilon)$. For $\varepsilon = 0.01$, this gives $\delta \approx 0.1$ — a much wider transition region than Example 1. The inner solution involves the error function rather than a pure exponential, reflecting the parabolic cylinder nature of the equation near the turning point.

10.3 Example 3: $a(x) = \cos x$, $b(x) = e^x$, $f(x) = x^2 + \sin x$

Problem Statement.

$$\varepsilon\,u''(x) + \cos(x)\,u'(x) + e^x\,u(x) = x^2 + \sin x, \quad u(0) = U_0, \quad u(1) = U_1.$$

10.3.1 Classification

Here $a(x) = \cos x \in [\cos 1, 1] \subset [0.54, 1]$ on $[0,1]$, so Assumption A2 holds with $\alpha_0 = \cos 1 \approx 0.5403$. The coefficient $b(x) = e^x > 0$ is positive (the simple maximum principle requires $b \le 0$; the problem is still uniquely solvable). The boundary layer is at $x = 0$ with thickness $\delta \approx \varepsilon/\cos(0) = \varepsilon$.

10.3.2 Outer Solution

Reduced equation ($\varepsilon = 0$):

$$\cos(x)\,u_0'(x) + e^x\,u_0(x) = x^2 + \sin x, \quad u_0(1) = U_1. \tag{E3.1}$$

Integrating factor:

$$\mu(x) = \exp\!\left(\int_0^x \frac{e^s}{\cos s}\,\mathrm{d}s\right) =: e^{M(x)}. \tag{E3.2}$$

$$\frac{d}{dx}\big[e^{M(x)}\,u_0\big] = e^{M(x)}\,\frac{x^2 + \sin x}{\cos x}. \tag{E3.3}$$

$$u_0(x) = e^{-M(x)}\left[\int_0^x e^{M(s)}\,\frac{s^2+\sin s}{\cos s}\,\mathrm{d}s + D\right], \tag{E3.4}$$

where D is fixed by $u_0(1) = U_1$.

10.3.3 Inner Correction

Near $x = 0$, $a(0) = \cos 0 = 1$. Setting $\xi = x/\varepsilon$:

$$v_0'' + 1 \cdot v_0' = 0 \implies v_0 = A_0 + B_0\, e^{-\xi}. \tag{E3.5}$$

Matching gives $A_0 = u_0(0)$, $B_0 = U_0 - u_0(0)$. Composite:

$$u(x) \approx u_0(x) + \big[U_0 - u_0(0)\big]\, e^{-x/\varepsilon} + O(\varepsilon). \tag{E3.6}$$

10.3.4 Higher-Order Outer Correction

The $O(\varepsilon)$ outer correction $u_1(x)$ satisfies $a\,u_1' + e^x\,u_1 = -u_0''$ with $u_1(1) = 0$.

$$u_1(x) = e^{-M(x)}\left[-\int_0^x e^{M(s)}\,\frac{u_0''(s)}{\cos s}\,\mathrm{d}s + D_1\right], \tag{E3.7}$$

with D_1 from $u_1(1) = 0$. Improved composite accurate to $O(\varepsilon^2)$:

$$u(x) \approx u_0(x) + \varepsilon\,u_1(x) + \big[U_0 - u_0(0) - \varepsilon(u_1(0) - v_1(0))\big]\, e^{-x/\varepsilon}. \tag{E3.8}$$

Observation 10.4. The combination of a trigonometric convection coefficient and exponential reaction makes the coefficient functions smooth but non-constant, preventing an exact closed form. The analysis demonstrates the full power of the matched asymptotic expansion: despite the lack of closed-form solutions, the structure of the boundary layer (exponential decay with rate $1/\varepsilon$, since $a(0) = 1$) is determined analytically, and the outer solution can be computed to any accuracy by numerical quadrature.

10.4 Example 4: $a(x) = 1+x$, $b(x) = x$, $f(x) = e^{-x}+\ln(1+x)$

Problem Statement.

$$\varepsilon\,u''(x) + (1+x)\,u'(x) + x\,u(x) = e^{-x} + \ln(1+x), \quad u(0) = U_0, \quad u(1) = U_1.$$

10.4.1 Classification and Key Observations

Here $a(x) = 1 + x \geq 1 > 0$ (Assumption A2 with $\alpha_0 = 1$), $b(x) = x \geq 0$, $f(x) = e^{-x} + \ln(1+x)$ (both smooth on $[0,1]$). The boundary layer is at $x = 0$ with thickness $O(\varepsilon/a(0)) = O(\varepsilon)$.

10.4.2 Outer Solution

$$(1+x)\,u_0'(x) + x\,u_0(x) = e^{-x} + \ln(1+x), \quad u_0(1) = U_1. \tag{E4.1}$$

Integrating factor:

$$\mu(x) = \exp\!\left(\int_0^x \frac{t}{1+t}\,\mathrm{d}t\right) = \exp\!\left(\int_0^x \left[1 - \frac{1}{1+t}\right]\,\mathrm{d}t\right) = \exp(x - \ln(1+x)) = \frac{e^x}{1+x}.$$

$$\frac{d}{dx}\left[\frac{e^x\,u_0}{1+x}\right] = \frac{e^x}{1+x}\cdot\frac{e^{-x} + \ln(1+x)}{1+x} = \frac{1}{(1+x)^2} + \frac{e^x\ln(1+x)}{(1+x)^2}. \tag{E4.2}$$

Integrating:

$$\frac{e^x\,u_0}{1+x} = \int_0^x \left[\frac{1}{(1+s)^2} + \frac{e^s\ln(1+s)}{(1+s)^2}\right]\,\mathrm{d}s + D. \tag{E4.3}$$

The first integral: $\displaystyle\int_0^x (1+s)^{-2}\,\mathrm{d}s = 1 - \frac{1}{1+x}$.

The second integral $I(x) = \displaystyle\int_0^x \frac{e^s\ln(1+s)}{(1+s)^2}\,\mathrm{d}s$ involves integration by parts; it is evaluated numerically. The outer solution is:

$$u_0(x) = (1+x)\,e^{-x}\left[1 - \frac{1}{1+x} + I(x) + D\right], \tag{E4.4}$$

with D determined from $u_0(1) = U_1$.

10.4.3 Inner Correction

At $x = 0$: $a(0) = 1$, $b(0) = 0$, $f(0) = 1$.

$$v_0'' + 1\cdot v_0' = 0 \implies v_0(\xi) = A_0 + B_0\,e^{-\xi}. \tag{E4.5}$$

Composite: $u(x) \approx u_0(x) + [U_0 - u_0(0)]\,e^{-x/\varepsilon} + O(\varepsilon)$.

10.4.4 Particular Solution via Power Series

Expanding:

$$e^{-x} = 1 - x + \frac{x^2}{2} - \frac{x^3}{6} + \cdots,$$
$$\ln(1+x) = x - \frac{x^2}{2} + \frac{x^3}{3} - \cdots,$$
$$f(x) = 1 + \frac{x^3}{6} - \frac{x^4}{12} + \cdots$$

Seek $u_p = a_0 + a_1 x + a_2 x^2 + \cdots$:

$$\text{Const}: \quad a_1 + 2\varepsilon\, a_2 = 1 \implies a_1 \approx 1,$$
$$x\text{-coeff}: \quad a_1 + 2a_2 + a_0 + 6\varepsilon\, a_3 = 0 \implies a_2 \approx (-1 - a_0)/2.$$

Observation 10.5. The logarithmic term $\ln(1+x)$ is bounded and smooth on $[0,1]$ (from 0 to $\ln 2 \approx 0.693$) and contributes non-algebraically to the particular solution. For small ε, the dominant outer behaviour is governed by the balance $(1+x)\,u_0' + x\,u_0 = e^{-x} + \ln(1+x)$.

10.5 Example 5: $a(x) = \sin x$, $b(x) = \cos x$, $f(x) = e^x + x^2$

Problem Statement.

$$\varepsilon\, u''(x) + \sin(x)\, u'(x) + \cos(x)\, u(x) = e^x + x^2, \quad u(0) = U_0, \quad u(1) = U_1.$$

10.5.1 Classification and Special Structure

Note the identity:

$$\frac{d}{dx}\big[\sin(x)\, u\big] = \cos(x)\, u + \sin(x)\, u'. \tag{E5.1}$$

Therefore $\sin(x)\, u' + \cos(x)\, u = \dfrac{d}{dx}[\sin(x)\, u]$. The full operator is:

$$L_\varepsilon[u] = \varepsilon\, u'' + \frac{d}{dx}\big[\sin(x)\, u\big]. \tag{E5.2}$$

Warning: $a(0) = \sin 0 = 0$, so this is again a turning-point problem. For x near 0, $\sin x \approx x$, and the boundary layer has width $O(\sqrt{\varepsilon})$.

10.5.2 Outer Solution

$$\frac{d}{dx}\big[\sin(x)\, u_0\big] = e^x + x^2, \quad u_0(1) = U_1. \tag{E5.3}$$

Integrating directly:

$$\sin(x)\,u_0(x) = \int_0^x (e^s + s^2)\,\mathrm{d}s + D = (e^x - 1) + \frac{x^3}{3} + D. \tag{E5.4}$$

Hence:

$$u_0(x) = \frac{(e^x - 1) + x^3/3 + D}{\sin x}, \quad x \in (0, 1]. \tag{E5.5}$$

Boundary condition $u_0(1) = U_1$ gives:

$$D = U_1 \sin(1) - (e - 1) - \tfrac{1}{3} \approx 0.8415\,U_1 - 2.0516.$$

10.5.3 Inner Solution

Near $x = 0$, $\sin x \approx x$ and $\cos x \approx 1$. Setting $\xi = x/\sqrt{\varepsilon}$:

$$\frac{\mathrm{d}^2 v_0}{\mathrm{d}\xi^2} + \xi\,\frac{\mathrm{d}v_0}{\mathrm{d}\xi} + v_0 = O(\sqrt{\varepsilon}). \tag{E5.6}$$

Using the identity $(\xi\,v_0)' = v_0 + \xi\,v_0'$, the leading-order equation is equivalent to $\left(\dfrac{d}{d\xi} + \xi\right)\dfrac{dv_0}{d\xi} = 0$, giving $\dfrac{dv_0}{d\xi} = A\,e^{-\xi^2/2}$ and $v_0(\xi) = A\displaystyle\int_0^\xi e^{-s^2/2}\,\mathrm{d}s + U_0$.

10.5.4 Particular Solution

Using the factored form (E5.2), the outer particular equation is:

$$\frac{d}{dx}\big[\sin(x)\,u_p\big] = e^x + x^2 \implies \sin(x)\,u_p = e^x + \frac{x^3}{3} + D_p.$$

$$u_p(x) = \frac{e^x + x^3/3 + D_p}{\sin x}. \tag{E5.7}$$

Choosing $D_p = -1$ (so numerator vanishes at $x = 0$):

$$u_p(x) = \frac{e^x - 1 + x^3/3}{\sin x}. \tag{E5.8}$$

For x near 0: $u_p \approx 1 + x/2 + x^2/3 + \cdots$.

Observation 10.6. The algebraic factorisation $\sin(x)\,u' + \cos(x)\,u = (\sin x \cdot u)'$ arises precisely when $b(x) = a'(x)$, since $(\sin x)' = \cos x = b(x)$. This exact-differential condition converts the outer equation to a simple quadrature (E5.4), giving an exact outer particular solution.

Chapter 11

Summary of Differential Equation Solutions

The following table consolidates the key analytical results from Chapter 10. For each example we record the boundary-layer thickness, the layer location, the nature of the inner scaling, and the form of the inner solution.

Table 11.1: Summary of boundary layer properties for Examples 1–5.

Ex.	$a(x)$	$b(x)$	Layer location	Thickness	Inner solution form
1	7	24	$x = 0$	$\delta = \varepsilon/7$	$C_2\, e^{-7x/\varepsilon}$ (pure exponential)
2	x	$x^2 + 1$	$x = 0$ (turning pt)	$O(\sqrt{\varepsilon})$	$A\ \mathrm{erf}\big(x/\sqrt{2\varepsilon}\big) + B$ (error function)
3	$\cos x$	e^x	$x = 0$	$\delta = \varepsilon$	$B\, e^{-x/\varepsilon}$ $(a(0) = 1)$
4	$1 + x$	x	$x = 0$	$\delta = \varepsilon$	$B\, e^{-x/\varepsilon}$ $(a(0) = 1)$
5	$\sin x$	$\cos x$	$x = 0$ (turning pt)	$O(\sqrt{\varepsilon})$	$A \int_0^{\xi} e^{-s^2/2}\, \mathrm{d}s + U_0$ (error function)

Chapter 12

Integral Equation Formulations

We now reformulate each of the five BVPs as an equivalent integral equation. The systematic procedure follows Section 9.5.1: (a) identify or construct the Green's function for the operator L_ε (or its simplified version $L_0 = \varepsilon D^2 + a(x)D$), and (b) write the solution as an integral against the Green's function. We then verify that solving the integral equation recovers the same solution as the ODE method.

12.1 General Procedure

For the operator $L_\varepsilon = \varepsilon D^2 + a(x)D + b(x)I$ with Dirichlet conditions, the Green's function $G(x,t)$ satisfies (9.5.1)–(9.5.2). The solution of the non-homogeneous problem (8.1.1)–(8.1.2) is given by the variation-of-parameters formula:

$$u(x) = c_1\phi_1(x) + c_2\phi_2(x) + \frac{1}{\varepsilon}\int_0^x \frac{\phi_1(t)\phi_2(x) - \phi_1(x)\phi_2(t)}{W(t)}\, f(t)\,\mathrm{d}t, \tag{12.1.1}$$

where $W(t) = \phi_1(t)\phi_2'(t) - \phi_2(t)\phi_1'(t)$ is the Wronskian. The boundary conditions then determine c_1 and c_2. The integral in (12.1.1) can be rewritten using (9.5.2) as

$$u(x) = h(x) + \int_0^1 G(x,t)\, f(t)\,\mathrm{d}t, \tag{12.1.2}$$

where $h(x)$ is the solution of the homogeneous BVP $L_\varepsilon[h] = 0$, $h(0) = U_0$, $h(1) = U_1$.

12.2 Example 1 — Constant Coefficients

12.2.1 Homogeneous Solutions

The homogeneous equation $\varepsilon\lambda^2 + 7\lambda + 24 = 0$ has roots λ_1, λ_2 from (E1.4). The standard choices satisfying $\phi_1(0) = 0$ and $\phi_2(1) = 0$ are:

$$\phi_1(x) = \frac{e^{\lambda_1 x} - e^{\lambda_2 x}}{\lambda_1 - \lambda_2}, \qquad \phi_2(x) = \frac{e^{\lambda_1(x-1)} - e^{\lambda_2(x-1)}}{\lambda_1 - \lambda_2}. \tag{12.2.1}$$

12.2.2 Wronskian Calculation

Using Abel's identity (9.4.2): $W(t) = W(0)\, e^{-7t/\varepsilon}$. Since $\phi_1(0) = 0$:

$$W(0) = \phi_1(0)\,\phi_2'(0) - \phi_2(0)\,\phi_1'(0) = -\phi_2(0).$$

For $\varepsilon = 0.01$, $\phi_2(0) \approx -e^{696.55}/693.1$ is exponentially large, reflecting the rapid growth of the boundary layer solution moving from $x = 1$ toward $x = 0$.

12.2.3 Green's Function for Example 1

Substituting into (9.5.2):

$$G(x,t) = \frac{\phi_1(x)\,\phi_2(t)}{\varepsilon\, W(t)}, 0 \le x \le t \le 1, \frac{\phi_1(t)\,\phi_2(x)}{\varepsilon\, W(t)}, 0 \le t \le x \le 1. \tag{12.2.2}$$

The exponential factor in $W(t) = W(0)\, e^{-7t/\varepsilon}$ cancels one of the exponentials in ϕ_1 or ϕ_2, producing a kernel $G(x,t)$ that is bounded uniformly in ε outside the boundary layer.

12.2.4 Integral Equation Solution

The solution is:

$$u(x) = h(x) + \int_0^1 G(x,t)\,(t + 2025)\,\mathrm{d}t, \tag{12.2.3}$$

where $h(x) = U_0\phi_2(x)/\phi_2(0) + U_1\phi_1(x)/\phi_1(1)$. For $U_0 = U_1 = 0$, $h(x) = 0$. Splitting and integrating using integration by parts:

$$\int_0^x e^{\lambda_1 t}(t + 2025)\,\mathrm{d}t = \frac{e^{\lambda_1 x}(x + 2025)}{\lambda_1} - \frac{e^{\lambda_1 x}}{\lambda_1^2} + \frac{2025}{\lambda_1} + \frac{1}{\lambda_1^2}.$$

After assembling all terms, the result is:

$$u(x) = C_1\, e^{\lambda_1 x} + C_2\, e^{\lambda_2 x} + \frac{x}{24} + \frac{48593}{576},$$

confirming exact agreement with the ODE solution (E1.7). This verifies Theorem 9.4 for Example 1.

12.3 Example 2 — Turning-Point Problem

For Example 2 ($a(x) = x$, $b(x) = x^2 + 1$), the homogeneous equation $\varepsilon\phi'' + x\phi' = 0$ gives $\phi' = A\,e^{-x^2/(2\varepsilon)}$, hence:

$$\phi(x) = A\int_0^x e^{-s^2/(2\varepsilon)}\,\mathrm{d}s + B.$$

The two solutions satisfying the boundary conditions are:

$$\phi_1(x) = \int_0^x e^{-s^2/(2\varepsilon)}\,\mathrm{d}s \quad (\phi_1(0) = 0),$$
$$\phi_2(x) = \int_x^1 e^{-s^2/(2\varepsilon)}\,\mathrm{d}s \quad (\phi_2(1) = 0).$$

Their sum $\phi_1(x) + \phi_2(x) = \Lambda(\varepsilon) := \displaystyle\int_0^1 e^{-s^2/(2\varepsilon)}\,\mathrm{d}s$. Wronskian:

$$W(x) = -\Lambda(\varepsilon)\,e^{-x^2/(2\varepsilon)}.$$

Green's function:

$$G(x,t) = \frac{\phi_1(x)\,\phi_2(t)}{\varepsilon\,\Lambda(\varepsilon)\,e^{-t^2/(2\varepsilon)}}, x \le t, \frac{\phi_1(t)\,\phi_2(x)}{\varepsilon\,\Lambda(\varepsilon)\,e^{-t^2/(2\varepsilon)}}, x \ge t.$$

The integral equation for Example 2 is:

$$u(x) + \int_0^1 G(x,t)\,(t^2+1)\,u(t)\,\mathrm{d}t = h(x) + \int_0^1 G(x,t)\sin t\,\mathrm{d}t. \tag{12.3.1}$$

This is a Fredholm equation of the second kind with kernel $K(x,t) = G(x,t)(t^2+1)$.

12.4 Example 3 — Trigonometric/Exponential Coefficients

For Example 3, the homogeneous equation $\varepsilon\phi'' + \cos(x)\,\phi' = 0$ gives $\phi' = A\,e^{-\sin(x)/\varepsilon}$, and

$$\phi(x) = A\int_0^x e^{-\sin(s)/\varepsilon}\,\mathrm{d}s + B =: A\,\Phi(x) + B, \tag{12.4.1}$$

where $\Phi(x) = \displaystyle\int_0^x e^{-\sin(s)/\varepsilon}\,\mathrm{d}s$. The two solutions are:

$$\phi_1(x) = \Phi(x), \quad \phi_2(x) = \Phi(1) - \Phi(x).$$

Wronskian: $W(x) = -\Phi(1)\, e^{-\sin(x)/\varepsilon}$.

$$G(x,t) = \frac{\Phi(x)\,[\Phi(1)-\Phi(t)]}{\varepsilon\,\Phi(1)\,e^{-\sin(t)/\varepsilon}}, x \le t, \frac{\Phi(t)\,[\Phi(1)-\Phi(x)]}{\varepsilon\,\Phi(1)\,e^{-\sin(t)/\varepsilon}}, x \ge t. \tag{12.4.2}$$

The full integral equation is:

$$u(x) + \int_0^1 G(x,t)\,e^t\,u(t)\,\mathrm{d}t = h(x) + \int_0^1 G(x,t)\,(t^2 + \sin t)\,\mathrm{d}t. \tag{12.4.3}$$

12.5 Example 4 — Variable Linear Coefficients

For $a(x) = 1 + x$, the homogeneous equation $\varepsilon\phi'' + (1+x)\phi' = 0$ gives $\phi' = A\,e^{-(x+x^2/2)/\varepsilon}$, hence:

$$\phi(x) = A\int_0^x e^{-(s+s^2/2)/\varepsilon}\,\mathrm{d}s + B =: A\,\Psi(x) + B. \tag{12.5.1}$$

Standard Laplace method gives $\Psi(\infty) \approx \varepsilon$ as $\varepsilon \to 0$.

$$\phi_1(x) = \Psi(x), \quad \phi_2(x) = \Psi(1) - \Psi(x), \quad W(x) = -\Psi(1)\,e^{-(x+x^2/2)/\varepsilon}.$$

$$G(x,t) = \frac{\Psi(x)\,[\Psi(1)-\Psi(t)]}{\varepsilon\,\Psi(1)\,e^{-(t+t^2/2)/\varepsilon}}, x \le t, \frac{\Psi(t)\,[\Psi(1)-\Psi(x)]}{\varepsilon\,\Psi(1)\,e^{-(t+t^2/2)/\varepsilon}}, x \ge t. \tag{12.5.2}$$

Integral equation:

$$u(x) + \int_0^1 G(x,t)\,t\,u(t)\,\mathrm{d}t = h(x) + \int_0^1 G(x,t)\,[e^{-t} + \ln(1+t)]\,\mathrm{d}t. \tag{12.5.3}$$

12.6 Example 5 — Exact-Differential Structure

The factorisation $L_\varepsilon = \varepsilon D^2 + D[\sin(x)\cdot]$ means we can write:

$$\frac{d}{dx}\left[\varepsilon\,\phi' + \sin(x)\,\phi\right] = 0 \implies \varepsilon\,\phi' + \sin(x)\,\phi = K \text{ (const)}. \tag{12.6.1}$$

Integrating factor $e^{-\cos x/\varepsilon}$:

$$\phi(x) = e^{\cos x/\varepsilon}\left[\frac{K}{\varepsilon}\int_0^x e^{-\cos s/\varepsilon}\,\mathrm{d}s + A\right]. \tag{12.6.2}$$

Two linearly independent solutions ($K = 0$, $A = 1$ and $K = 1$, $A = 0$):

$$\phi_h(x) = e^{\cos x/\varepsilon},$$
$$\phi_q(x) = e^{\cos x/\varepsilon} \int_0^x \frac{e^{-\cos s/\varepsilon}}{\varepsilon}\, \mathrm{d}s.$$

The Wronskian:

$$W(x) = \phi_h \phi_q' - \phi_q \phi_h' = e^{\cos x/\varepsilon} \cdot \frac{e^{-\cos x/\varepsilon}}{\varepsilon} = \frac{1}{\varepsilon} \quad \text{(constant!)}$$

This remarkable constancy reflects the exact-differential structure. The Green's function satisfies $\varepsilon\, W(t) = 1$, and:

$$G(x,t) = \phi_h(x)\, \phi_q(t) - \phi_q(x)\, \phi_h(t), x \le t, \phi_h(t)\, \phi_q(x) - \phi_q(t)\, \phi_h(x), x \ge t. \tag{12.6.3}$$

The integral equation is:

$$u(x) + \int_0^1 G(x,t)\, \cos(t)\, u(t)\, \mathrm{d}t = h(x) + \int_0^1 G(x,t)\, (e^t + t^2)\, \mathrm{d}t. \tag{12.6.4}$$

Observation 12.1. The constant Wronskian $W = 1/\varepsilon$ in Example 5 is a direct consequence of the exact-differential structure: the operator $L_\varepsilon = \varepsilon D^2 + (\sin x \cdot I)'$ is a sum of a pure second derivative and a pure first derivative (of a product). This structure yields a particularly clean Green's function formula.

Chapter 13

Comparison of Differential and Integral Equation Solutions

13.1 Formal Equivalence: Proof for the General Case

Theorem 13.1 (Equivalence of ODE and Integral Equation Solutions)**.** *Let $u_{\text{ODE}} \in C^2[0,1]$ be the unique solution of the BVP $L_\varepsilon[u] = f$, $u(0) = U_0$, $u(1) = U_1$. Let u_{IE} be the solution of the Fredholm integral equation* (12.1.2)*. Then $u_{\text{ODE}} = u_{\text{IE}}$ on $[0,1]$.*

Proof. (Direction 1: ODE $\Rightarrow$ IE.) Let $u = u_{\text{ODE}}$. Multiply $L_\varepsilon[u] = f$ by $G(x,t)$ and integrate over $t \in [0,1]$:

$$\int_0^1 G(x,t)\, L_\varepsilon[u](t)\, \mathrm{d}t = \int_0^1 G(x,t)\, f(t)\, \mathrm{d}t. \tag{13.1.1}$$

Integrate the left side by parts twice, using the adjoint boundary conditions $G(x,0) = G(x,1) = 0$ and $L_\varepsilon^*[G(x,\cdot)](t) = \delta(t-x)$:

$$\int_0^1 G(x,t)\, L_\varepsilon[u](t)\, \mathrm{d}t = \int_0^1 u(t)\, L_\varepsilon^*[G(x,\cdot)](t)\, \mathrm{d}t + [\text{boundary terms}] = u(x) + [\text{boundary terms}].$$

The boundary terms combine to give exactly $h(x)$, so (13.1.1) becomes:

$$u(x) = h(x) + \int_0^1 G(x,t)\, f(t)\, \mathrm{d}t,$$

i.e. u_{ODE} satisfies the integral equation, hence $u_{\text{ODE}} = u_{\text{IE}}$.

(Direction 2: IE $\Rightarrow$ ODE.) Differentiate (12.1.2) twice with respect to x. The jump condition $[\partial G/\partial x]_{x=t^+} - [\partial G/\partial x]_{x=t^-} = 1/\varepsilon$ (from (9.5.1)) produces the delta function upon differentiation, recovering $L_\varepsilon[u] = f$. The boundary conditions $u(0) = U_0$, $u(1) =$

U_1 follow from $G(0,t) = G(1,t) = 0$ and $h(0) = U_0$, $h(1) = U_1$. □

13.2 Example-by-Example Verification

13.2.1 Example 1: Direct Verification

For Example 1, both methods produce:

$$u(x) = C_1\, e^{\lambda_1 x} + C_2\, e^{\lambda_2 x} + \frac{x}{24} + \frac{48593}{576},$$

with the same constants C_1, C_2 determined by the same boundary conditions. The identification is exact: the variation-of-parameters integral formula (12.1.1) with the constant-coefficient fundamental solutions reduces to the same two exponentials plus the polynomial particular integral.

13.2.2 Numerical Comparison ($\varepsilon = 0.01$, Example 1)

Table 13.1: Solution comparison at $x = 0.5$ for Example 1 ($U_0 = U_1 = 0$, $\varepsilon = 0.01$).

Method	$u(0.5)$	Error	Remarks
DE (exact)	$u_p(0.5) \approx 84.42$	0	Reference
IE (exact)	$u(0.5) \approx 84.42$	0	$\equiv$ ODE
Composite (9.3.6)	$u_{\text{comp}}(0.5) \approx 84.42$	$O(\varepsilon) < 1\%$	Layer≈ 0
ODE vs IE	$u_{\text{ODE}} - u_{\text{IE}} = 0$	0	Identical
Comp. vs exact	$u_{\text{comp}} - u_{\text{exact}} \approx 0$	$O(\varepsilon) < 1\%$	Asymptotic

13.3 Stability and Convergence Analysis

For the Fredholm equation (9.5.4), the Neumann series solution $u = \sum_{n=0}^{\infty} T^n[g]$ (where T is the integral operator with kernel $-G_0(x,t)\, b(t)$) converges whenever the spectral radius $\rho(T) < 1$. The operator norm satisfies:

$$\|T\| \;\le\; \|b\|_\infty \cdot \|G_0\|_{L^1} \;\le\; \frac{\|b\|_\infty \cdot C(a,\varepsilon)}{\alpha_0}, \tag{13.3.1}$$

where $C(a,\varepsilon)$ is bounded uniformly in ε for non-turning-point problems.

For Example 1 (constant coefficients), $\|G_0\| = O(\varepsilon/7)$, so $\|T\| = 24 \times O(\varepsilon/7) = O(\varepsilon) \to 0$ as $\varepsilon \to 0$. The Neumann series therefore converges rapidly for small ε, with the n-th term bounded by $O(\varepsilon^n)$.

For turning-point problems (Examples 2 and 5), the operator norm is $O(\sqrt{\varepsilon})$ rather than $O(\varepsilon)$, so convergence is slower but still guaranteed for sufficiently small ε.

Chapter 14

Discussion

14.1 Advantages of the Differential Equation Approach

The direct ODE method has several practical strengths.

1. For constant-coefficient problems (Example 1), it yields exact closed-form solutions expressible in terms of elementary functions.
2. The method is computationally straightforward: the characteristic equation is algebraic, particular solutions are found by undetermined coefficients or variation of parameters, and boundary conditions yield a simple 2×2 linear system.
3. The asymptotic structure of the solution (the slow and fast roots λ_1, λ_2 with $\lambda_2 = O(1/\varepsilon)$) is immediately transparent from the characteristic equation, giving direct insight into the boundary layer thickness and location.
4. Higher-order asymptotic corrections are systematically generated by the matched asymptotic expansion, with each correction satisfying an explicit first-order ODE.

The primary disadvantage is that for variable-coefficient problems (Examples 3–5), the homogeneous solutions are not expressible in closed form. Standard ODE solvers (Runge–Kutta) fail due to stiffness (the stiffness ratio $\lambda_2/\lambda_1 = O(1/\varepsilon)$ can be 10^4 for $\varepsilon = 0.01$), requiring implicit solvers or exponential time-stepping. Finite difference discretisation on uniform meshes produces spurious oscillations when $h > \varepsilon$, necessitating mesh refinement or upwinding.

14.2 Advantages of the Integral Equation Approach

The integral equation reformulation offers complementary strengths. The boundary conditions are embedded in the Green's function and the harmonic interpolant $h(x)$, reducing

the two-point boundary value problem to an unconstrained integral equation on $[0, 1]$.

The compactness of the integral operator T in $C[0, 1]$ (it maps bounded continuous functions to equicontinuous families by the Arzelà–Ascoli theorem) guarantees convergence of approximation methods that might not converge for the stiff ODE. The Neumann series solution provides a constructive existence proof and a convergence rate estimate ($O(\varepsilon^n)$ per n iterations for small ε). Furthermore, the Fredholm framework admits elegant functional-analytic tools: the Fredholm alternative, spectral theory, and the theory of compact operators.

A disadvantage is the computational cost: whereas the ODE finite difference system is tridiagonal ($O(N)$ operations for N mesh points), the full Fredholm system is dense ($O(N^2)$ storage and $O(N^2)$ or $O(N^3)$ operations).

14.3 Computational Complexity Comparison

Table 14.1: Comparison of ODE and integral equation methods.

Criterion	**ODE Method**	**IE Method**
Storage	$O(N)$ tridiagonal	$O(N^2)$ dense matrix
Direct solver cost	$O(N)$ (Thomas alg.)	$O(N^3)$ (Gaussian elim.)
Condition number (uniform mesh, small ε)	$O(1/\varepsilon)$	$O(1)$ or $O(1/\sqrt{\varepsilon})$
Accuracy on uniform mesh	$O(h)$ or $O(h^2)$, requires $h \ll \varepsilon$	$O(h^p)$ for any h with p-point quadrature
Layer-adapted mesh needed?	Yes (Shishkin or Bakhvalov)	No (kernel smoothes layer)
Convergence theory	Classical ODE stability	Fredholm compact-operator theory

14.4 Physical Interpretation of Boundary Layer Behaviour

From a physical standpoint, the boundary layer in singularly perturbed convection–diffusion problems represents a thin region near a boundary where diffusive effects, though small globally, must balance the finite flux imposed by the boundary condition. Outside the layer, the balance is between convection (advection) and reaction, giving the slow outer solution u_0. Inside the layer, diffusion ($\varepsilon\, u''$) is the same order as convection ($a(0)\, u'$), producing the rapid exponential adjustment.

Increasing ε widens the layer (more diffusion) and smooths the solution; decreasing ε sharpens it. In the limit $\varepsilon \to 0$, the boundary layer becomes a jump discontinuity in the derivative at $x = 0$ — the outer solution u_0 satisfies $u_0(0) \neq U_0$ in general, and the layer 'concentrates' the derivative jump at a single point.

This is the mathematical analogue of the physical phenomenon of a very thin viscous sublayer in a turbulent boundary layer flow, or the skin depth in high-frequency electromagnetic wave propagation, or the penetration depth of a reactant in a fast heterogeneous reaction at a catalytic surface.

14.5 Effect of the Large Constant 2025 in Example 1

The choice $f(x) = x+2025$ was made to include a large constant term. This illustrates an important physical point: when the source (forcing) term is large, the particular solution dominates the homogeneous solution, and the boundary layer correction $[U_0 - u_0(0)]\, e^{-7x/\varepsilon}$ is a small fraction of the total solution magnitude, even though it varies on the fast scale ε. In numerical computations, this means the relative error due to neglecting the boundary layer may be small even on a coarse mesh, but the absolute error near $x = 0$ could still be significant if $U_0 \neq u_0(0)$.

14.6 Conclusion

Overview of the Study

This dissertation has presented a comprehensive and rigorous mathematical investigation into the relationship between linear second-order boundary value problems (BVPs) and their equivalent integral equation formulations, with particular emphasis on singularly perturbed problems arising in applied mathematics. The work spans two interrelated themes: first, the classical equivalence between a differential BVP and its corresponding Fredholm integral representation via the Green's function; and second, the asymptotic and functional-analytic theory of singularly perturbed convection–diffusion–reaction equations of the form

$$\varepsilon\, u''(x) + a(x)\, u'(x) + b(x)\, u(x) = f(x), \qquad 0 \leq x \leq 1, \quad u(0) = U_0, \quad u(1) = U_1, \tag{14.6.1}$$

where $\varepsilon > 0$ is a small parameter. Together, these themes establish a unified analytical and computational framework in which differential and integral equation methods are shown to be theoretically equivalent, practically complementary, and mutually reinforcing.

Analytical Formulation and the Green's Function Approach

The point of departure was the classical model problem

$$u''(x) = x + 1, \quad 0 \le x \le 1, \qquad u(0) = 0,\ u(1) = 0,$$

solved in closed form by direct integration, yielding the exact analytical solution

$$u(x) = \frac{x^3 + 3x^2 - 4x}{6}.$$

The same problem was then reformulated as a Fredholm integral equation of the second kind via the Green's function

$$G(x,s) = \begin{cases} (1-s)\,x, & 0 \le x \le s, \\ s\,(1-x), & s \le x \le 1, \end{cases}$$

associated with the operator $\mathcal{L}[u] = u''$ under homogeneous Dirichlet boundary conditions. The resulting integral representation

$$u(x) = \int_0^1 G(x,s)\,(s+1)\,\mathrm{d}s$$

was evaluated analytically by splitting the domain at $x = s$ and computing each part explicitly. The result was shown to coincide exactly with the direct ODE solution, thereby establishing the equivalence of the two formulations for this canonical example.

A second model problem,

$$y''(x) + 2\,y(x) = x, \quad 0 < x < 1, \qquad y(0) = 1,\ y(1) = 0,$$

with non-homogeneous boundary conditions was treated by a lifting transformation $y(x) = u(x) + H(x)$, where $H(x) = 1 - x$ is the harmonic interpolant satisfying the boundary conditions. The reduced problem for u was then cast as a Fredholm integral equation with kernel $G(x,t)$ and free term $f_0(x) = -\frac{1}{2}x(1-x)^2$. By uniqueness of the solution, the Fredholm formulation was verified to reproduce the ODE solution

$$y_{\mathrm{ODE}}(x) = \cos\!\big(\sqrt{2}\,x\big) - \frac{\cos(\sqrt{2}) + \frac{1}{2}}{\sin(\sqrt{2})}\sin\!\big(\sqrt{2}\,x\big) + \frac{x}{2},$$

confirming the theoretical equivalence in a non-trivial setting with a non-zero reaction term. This equivalence is not accidental: it is a consequence of the fact that the Green's function $G(\cdot,t)$ satisfies $\mathcal{L}_\varepsilon[G(\cdot,t)](x) = \delta(x-t)$ in the distributional sense, so that applying the operator $\mathcal{L}_\varepsilon$ to the integral representation recovers the original differential

equation, while integration by parts in the reverse direction recovers the integral equation from the differential one (Theorems 10.4 and 14.1).

Numerical Experiments and Computational Verification

Alongside the analytical developments, extensive numerical experiments were conducted in MATLAB to corroborate the theoretical findings. Three independent numerical approaches were implemented and compared:

1. **MATLAB `bvp4c` solver**: a collocation method with residual control, which produced solutions agreeing with the exact analytical expressions to within machine precision ($\sim 10^{-6}$–10^{-8}) for both model problems.
2. **Fredholm integral quadrature**: the trapezoidal rule applied to the integral representation on a uniform grid of 2000 points reproduced the exact solution with errors of the same order of magnitude.
3. **Finite difference discretisation**: a standard second-order centred scheme on a coarse grid of $N = 5$ subintervals was applied to the second model problem, yielding nodal values in close agreement with the exact solution and demonstrating even the basic scheme's practical adequacy for smooth problems.

Graphical comparisons confirmed the visual indistinguishability of the three solution profiles from the exact analytical curve across the full interval $[0, 1]$. These numerical experiments reinforce the conclusion that the Green's function/integral equation approach is not merely a theoretical reformulation but a computationally robust alternative that, in many settings, offers superior conditioning relative to the differential equation discretisation.

Singular Perturbation Theory and Boundary Layer Analysis

The second and more advanced part of this dissertation addressed the singularly perturbed problem (14.6.1). When $\varepsilon \ll 1$, the solution exhibits a sharp boundary layer of thickness $O(\varepsilon/a(0))$ near $x = 0$ (when $a(x) > 0$), in which the solution transitions rapidly from the imposed boundary value U_0 to the slowly varying outer solution $u_0(x)$. The outer solution satisfies the reduced first-order equation $a(x)\,u_0' + b(x)\,u_0 = f(x)$ with right-end condition $u_0(1) = U_1$, while the inner solution, expressed in the stretched coordinate $\xi = x/\varepsilon$, takes the form $v_0(\xi) = A_0 + B_0\,e^{-a(0)\xi}$. The composite uniformly valid approximation

$$u_{\text{comp}}(x) = u_0(x) + \big[U_0 - u_0(0)\big]\,e^{-a(0)x/\varepsilon} + O(\varepsilon)$$

captures both the outer behaviour and the boundary layer correction in a single, closed-form formula, uniformly valid on $[0, 1]$ in the supremum norm.

A rigorous stability analysis (Theorem 10.1) provided ε-uniform bounds on the solution and its derivative:

$$\|u\|_\infty \le \max\{|U_0|, |U_1|\} + \frac{1}{\alpha_0}\|f\|_\infty, \qquad |u'(x)| \le C_1\big(1 + \varepsilon^{-1}e^{-\alpha_0 x/\varepsilon}\big)\,,$$

quantifying the sharp exponential variation in the boundary layer. The existence and uniqueness of the solution for every $\varepsilon > 0$ was established via Abel's identity for the Wronskian of the homogeneous equation and the invertibility of the resulting 2×2 boundary condition system (Theorem 10.3).

Five Worked Examples: Diversity of Solution Structures

To illustrate the breadth of the theory, five BVPs with qualitatively distinct coefficient functions were analysed in full, and each was subsequently reformulated as a Fredholm integral equation. The results are summarised as follows.

- **Example 1** ($a = 7$, $b = 24$, $f(x) = x + 2025$): Constant coefficients yield an exact closed-form solution in terms of two exponentials $e^{\lambda_1 x}$ and $e^{\lambda_2 x}$, where $\lambda_2 \approx -7/\varepsilon$ is the fast boundary-layer root. The large constant 2025 in the forcing function ensures that the particular solution $u_p(0) \approx 84.4$ dominates the homogeneous component, illustrating how the relative magnitude of the boundary-layer correction depends on the amplitude of the forcing term.

- **Example 2** ($a(x) = x$, $b(x) = x^2 + 1$, $f(x) = \sin x$): The vanishing of $a(0) = 0$ defines a *turning-point problem*. The inner scaling is $\xi = x/\sqrt{\varepsilon}$, yielding a Weber (parabolic cylinder) equation whose solution involves the error function $\mathrm{erf}(\xi/\sqrt{2})$. The boundary layer width is $O(\sqrt{\varepsilon})$, an order of magnitude wider than in the non-turning-point cases.

- **Example 3** ($a(x) = \cos x$, $b(x) = e^x$): Variable trigonometric and exponential coefficients preclude closed-form fundamental solutions; the outer solution is expressed via a non-elementary integral over the integrating factor $e^{M(x)}$ where $M(x) = \int_0^x e^s/\cos s \,\mathrm{d}s$.

- **Example 4** ($a(x) = 1 + x$, $b(x) = x$, $f(x) = e^{-x} + \ln(1 + x)$): The logarithmic source term contributes a non-algebraic particular solution evaluated through integration by parts, demonstrating the technique's applicability beyond polynomial and trigonometric forcing.

- **Example 5** ($a(x) = \sin x$, $b(x) = \cos x$): The identity $\sin(x)\,u' + \cos(x)\,u = \frac{d}{dx}[\sin(x)\,u]$ reveals an *exact-differential structure*, converting the outer equation to a direct quadrature. The corresponding Wronskian is constant ($W \equiv 1/\varepsilon$), pro-

ducing a particularly clean Green's function, and the turning-point character at $x = 0$ again requires the $\sqrt{\varepsilon}$ inner scaling.

For each example, the integral equation reformulation was constructed explicitly, and Theorem 14.1 established that the ODE and integral equation solutions are identical. The Neumann series for the Fredholm operator converges at rate $O(\varepsilon^n)$ per iteration in non-turning-point cases and $O(\varepsilon^{n/2})$ in turning-point cases, confirming rapid convergence for small ε.

Equivalence of Differential and Integral Formulations

The central theoretical result of this dissertation is the rigorous proof that the differential equation BVP and the Fredholm integral equation

$$u(x) = h(x) + \int_0^1 G(x,t)\, f(t)\, \mathrm{d}t$$

are fully equivalent formulations of the same boundary value problem (Theorems 10.4 and 14.1). In the forward direction, applying $\mathcal{L}_\varepsilon$ to the integral representation and using the distributional identity $\mathcal{L}_\varepsilon[G(\cdot,t)](x) = \delta(x-t)$ recovers the differential equation with the correct boundary conditions. In the reverse direction, multiplying the differential equation by $G(x,t)$, integrating by parts twice, and invoking the adjoint boundary conditions for G recovers the integral representation. This bidirectional equivalence guarantees that no information is lost in the transformation and that the two formulations share a unique solution.

The practical consequences of this equivalence are significant. The integral equation formulation embeds the boundary conditions into the Green's function and the harmonic interpolant $h(x)$, removing the need to impose them as separate algebraic constraints. The resulting integral operator $\mathcal{T}[u](x) = \int_0^1 G(x,t)\, b(t)\, u(t)\, \mathrm{d}t$ is compact on $C[0,1]$ by the Arzelà–Ascoli theorem, making Fredholm theory and spectral analysis directly applicable. Moreover, the smoothing action of the integral operator mitigates the stiffness inherent in the differential formulation, enabling uniform convergence of quadrature-based methods on uniform meshes — an important advantage over finite difference schemes, which require layer-adapted (Shishkin or Bakhvalov) meshes to achieve ε-uniform accuracy.

Practical Applications

The mathematical framework developed in this dissertation is not merely of theoretical interest; it underpins the analysis of a wide range of physical and engineering problems. In *fluid mechanics*, the singularly perturbed convection–diffusion equation models the transport of momentum or scalars at high Reynolds or Péclet numbers, with

$\varepsilon = 1/\mathrm{Re}$ or $\varepsilon = 1/\mathrm{Pe}$; the boundary layer at the solid wall corresponds precisely to the Prandtl viscous sublayer. In *heat transfer*, the steady-state advection–diffusion equation $\varepsilon T'' - a(x)T' = S(x)$ governs the temperature distribution in channel flows dominated by convection, with a thin thermal boundary layer of thickness $O(1/\mathrm{Pe})$ at the inlet. In *quantum mechanics*, the time-independent Schrödinger equation in the semiclassical limit $\hbar \to 0$ takes precisely the form (14.6.1), with the WKB approximation corresponding to the matched asymptotic expansion; exponentially decaying inner solutions correspond to quantum tunnelling through classically forbidden regions. In *optimal control theory*, the cheap-control limit $\varepsilon \to 0$ of the linear-quadratic regulator yields a singularly perturbed two-point BVP whose boundary layers represent rapid initial and terminal transients in the optimal trajectory. Last but not least, stiff kinetics in reaction–diffusion systems having rate constants of order $1/\varepsilon$ generate concentrated profiles that have sharp inner or boundary layers located at the reactive boundaries, and in this case the integral equation framework naturally leads to the construction and study of concentrated profiles.

Significance of the Matched Asymptotic and Green's Function Approaches

Matched asymptotic expansions together with the Green's function method comprise the two main analytical techniques of this dissertation, and their complementary nature should be stressed. The matched asymptotic approach is local in nature. It splits the solution into an outer region described by the reduced equation and an inner boundary-layer region described by a rescaled equation and glues these two regions together via an asymptotic matching principle. Its main virtue is physical insight - the location, extent and decay rate of the boundary layer are directly found from $a(x)$ at $x = 0$ and the composite expression (14.6.1) gives an explicit, uniformly valid approximation with $O(\varepsilon)$ accuracy bounds.

By contrast, the Green's function method is a global method-it provides a single integral of the solution over the domain, where the boundary data are baked in intrinsically. Its appeal is in its functional-analytic simplicity-the solution map $f \mapsto u$ can be written as a bounded linear operator on a Banach space, and Fredholm alternative, spectral theory, and ε-perturbation theory are at one's fingertips. We gave a constructive proof of existence and transparent error estimates through the resolvent Neumann series. And through compact operator theory, we guaranteed that Galerkin, Collocation and Nyström discretization converge independent of stiffness ε.

Future Research Directions

The results presented in this dissertation open several avenues for further investigation.

Nonlinear singular perturbation problems. This analysis for the linear equation (14.6.1) may be generalized for the nonlinear case $\varepsilon u'' + f(x, u, u') = 0$, if the nonlinearity f verifies a Lipschitz condition. For small enough ε the existence and uniqueness of the fixed point of the associated nonlinear Fredholm equation is ensured by Banach contraction mapping theorem, and the speed of convergence of the Picard iteration may be bounded with the norm of operator: $\|\mathcal{T}\| = O(\varepsilon)$.

Systems and matrix Green's functions. The system of vector extension $\varepsilon \mathbf{U}'' + A(x)\mathbf{U}' + B(x)\mathbf{U} = \mathbf{F}(x)$ is Fredholm and has a matrix Green's function. The boundary-layer behavior depends on the eigenvalues of $A(0)$ and $A(1)$ and when A has positive and negative eigenvalues there will be layers at both endpoints and a complicated set of conditions to match the approximate solution together.

ε-uniform numerical quadrature. A practically important open problem is the development of quadrature rules for the Fredholm integral equation that are uniformly accurate in ε, exploiting the explicit ε-dependence of the Green's function kernel. Standard composite trapezoidal or Gauss quadrature achieves $O(h^p)$ accuracy for fixed ε but may require $h \ll \varepsilon$ to resolve the kernel's rapid variation near $t = x$. Modified Gaussian rules that incorporate the exponential weight $e^{-a(0)|x-t|/\varepsilon}$ could yield ε-robust high-order accuracy on uniform meshes.

Turning-point problems and Stokes phenomena. The systematic analysis of problems where $a(x_0) = 0$ at an interior point requires WKB or parabolic cylinder inner expansions, and the connection formulae across the turning point (Stokes phenomena, analogous to the quantum mechanics tunnelling problem) involve exponentially small corrections beyond all orders in ε. This is an active area of research with deep connections to the theory of resurgence and trans-series.

Sensitivity analysis and uncertainty quantification. The sensitivity of the solution to variations in ε can be quantified via

$$\frac{\partial u}{\partial \varepsilon}(x) = \int_0^1 \frac{\partial G}{\partial \varepsilon}(x, t)\, f(t)\, \mathrm{d}t + \frac{\partial h}{\partial \varepsilon}(x),$$

where $\partial G/\partial \varepsilon$ can be computed from the ε-derivative of the homogeneous fundamental solutions. Such sensitivity estimates are directly relevant to uncertainty quantification in fluid mechanics, where $\varepsilon = 1/\mathrm{Re}$ may itself be uncertain, and to robust control design with imperfectly known system parameters.

Closing Remarks

The overall result of this thesis is both obvious and profound. If a linear boundary value problem is posed either as a differential equation or as an equivalent Fredholm integral equation, then one is essentially discussing the same unique mathematical object-the solution-in two entirely equivalent, but different, languages. It is the Green's function which provides the exact dictionary between these two languages: it lumps together the differential operator and boundary data and the delta function source, so that the resultant kernel is one that encapsulates simultaneously both the integral operator and a formula for its solution. Singularly perturbed problems are problems where this analogy takes on added weight. Small parameter, in a sense, does not make a different problem but rather one of two scales, one diffusive, of size co, the other convective, of size unity; matched asymptotic expansions (formal methods) andFredholm integral equations (functional-analytic methods) provide the two vocabularies for this two-scale problem, and, as has been demonstrated throughout this thesis, both return the same unique solution.Mastery of both languages, and understanding their equivalence, constitutes the essential mathematical competence for the rigorous and efficient treatment of boundary value problems that arise throughout applied mathematics, physics, and engineering.

Bibliography

[1] Allen, D.N. de G. and Southwell, R.V. (1955). Relaxation methods applied to determine the motion, in two dimensions, of a viscous fluid past a fixed cylinder. *Quarterly Journal of Mechanics and Applied Mathematics*, 8(2), pp. 129–145.

[2] Bender, C.M. and Orszag, S.A. (1999). *Advanced Mathematical Methods for Scientists and Engineers I: Asymptotic Methods and Perturbation Theory*. Springer, New York.

[3] Cakir, M. and Amiraliyev, G.M. (2002). A numerical method for a singularly perturbed three-point boundary value problem. *Journal of Applied Mathematics*, 2010, Article 495184.

[4] De Jager, E.M. and Furu, J. (1996). *The Theory of Singular Perturbations*. Elsevier, Amsterdam.

[5] Farrell, P.A., Hegarty, A.F., Miller, J.J.H., O'Riordan, E. and Shishkin, G.I. (2000). *Robust Computational Techniques for Boundary Layers*. CRC Press / Chapman & Hall, Boca Raton.

[6] Friedrichs, K.O. (1955). Asymptotic phenomena in mathematical physics. *Bulletin of the American Mathematical Society*, 61(6), pp. 485–504.

[7] Il'in, A.M. (1969). Differencing scheme for a differential equation with a small parameter affecting the highest derivative. *Mathematical Notes of the Academy of Sciences of the USSR*, 6(2), pp. 596–602.

[8] Kadalbajoo, M.K. and Aggarwal, V.K. (2005). Fitted mesh B-spline collocation method for solving self-adjoint singularly perturbed boundary value problems. *Applied Mathematics and Computation*, 161(3), pp. 973–987.

[9] Kaplun, S. (1954). The role of coordinate systems in boundary-layer theory. *Zeitschrift für Angewandte Mathematik und Physik*, 5(2), pp. 111–135.

[10] Kevorkian, J. and Cole, J.D. (1996). *Multiple Scale and Singular Perturbation Methods*. Springer, New York.

[11] Kress, R. (1989). *Linear Integral Equations*. Springer, Berlin.

[12] Miller, J.J.H., O'Riordan, E. and Shishkin, G.I. (1996). *Fitted Numerical Methods for Singular Perturbation Problems: Error Estimates in the Maximum Norm for Linear Problems in One and Two Dimensions*. World Scientific, Singapore.

[13] Mohapatra, J. and Natesan, S. (2009). Parameter-uniform numerical method for global solution and global normalized flux of singularly perturbed boundary value problems using grid equidistribution. *Computers & Mathematics with Applications*, 60(7), pp. 1924–1939.

[14] Nayfeh, A.H. (1981). *Introduction to Perturbation Techniques*. Wiley-Interscience, New York.

[15] O'Malley, R.E. (1991). *Singular Perturbation Methods for Ordinary Differential Equations*. Springer, New York.

[16] Prandtl, L. (1904). Über Flüssigkeitsbewegung bei sehr kleiner Reibung. In: *Verhandlungen des III. Internationalen Mathematiker-Kongresses, Heidelberg*, pp. 484–491. Teubner, Leipzig.

[17] Roos, H.-G., Stynes, M. and Tobiska, L. (2008). *Robust Numerical Methods for Singularly Perturbed Differential Equations*. 2nd edn. Springer, Berlin.

[18] Shishkin, G.I. (1990). Grid approximation of singularly perturbed elliptic and parabolic equations. Doctoral thesis, Keldysh Institute of Applied Mathematics, Moscow (in Russian).

[19] Stakgold, I. and Holst, M. (2011). *Green's Functions and Boundary Value Problems*. 3rd edn. Wiley, Hoboken, NJ.

[20] Van Dyke, M. (1964). *Perturbation Methods in Fluid Mechanics*. Academic Press, New York.

[21] Verhulst, F. (2005). *Methods and Applications of Singular Perturbations: Boundary Layers and Multiple Timescale Dynamics*. Springer, New York.

[22] Wasow, W. (1965). *Asymptotic Expansions for Ordinary Differential Equations*. Wiley-Interscience, New York.

[23] Ames, W. F. *Numerical Methods for Partial Differential Equations*. Academic Press, 1992.

[24] Arfken, G., Weber, H. J., and Harris, F. *Mathematical Methods for Physicists*. 7th ed. Academic Press, 2013.

[25] Atkinson, K. E. *The Numerical Solution of Integral Equations of the Second Kind*. Cambridge University Press, 1997.

[26] Atkinson, K. E., and Han, W. *Theoretical Numerical Analysis: A Functional Analysis Framework*. Springer, 2009.

[27] Shampine, L. F., Kierzenka, J., and Reichelt, M. Solving Boundary Value Problems for Ordinary Differential Equations in MATLAB Using `bvp4c`. *MathWorks Technical Report*, 2000.

[28] Stakgold, I., and Holst, M. *Green's Functions and Boundary Value Problems*. 3rd ed. Wiley-Interscience, 2011.

[29] Tricomi, F. G. *Integral Equations*. Dover Publications, 1985.

[30] Courant, R., and Hilbert, D. *Methods of Mathematical Physics*, Vol. II. Wiley-VCH, 1989.

[31] Smith, G. D. *Numerical Solution of Partial Differential Equations: Finite Difference Methods*. Oxford University Press, 1985.

[32] Boyce, W. E., and DiPrima, R. C. *Elementary Differential Equations and Boundary Value Problems*. 10th ed. Wiley, 2012.

[33] Press, W., Teukolsky, S., Vetterling, W., and Flannery, B. *Numerical Recipes: The Art of Scientific Computing*. Cambridge University Press, 2007.

[34] MathWorks Documentation. *MATLAB R2023b: Boundary Value Problems*. Available online: `https://www.mathworks.com/help/matlab/ref/bvp4c.html`

[35] Polyanin, A. D., and Manzhirov, A. V. *Handbook of Integral Equations*. 2nd ed. CRC Press, 2008.

DELHI TECHNOLOGICAL UNIVERSITY

(Formerly Delhi College of Engineering)

Shahbad Daulatpur, Main Bawana Road, Delhi-42

PLAGIARISM VERIFICATION

Title of the Thesis: A Study of a Boundary Value Problem and Its Equivalent Fredholm / Volterra Integral Equation Formulation

Total Pages: 86 **Name of the Scholar:** Sudhanshu Ranjan

Supervisor(s): Prof. Dr. Vivek Aggarwal

Department: Department of Applied Mathematics

This is to report that the above thesis was scanned for similarity detection. Process and outcome is given below:

Similarity Index:9%

Software used: Turnitin

Total Word Count: 17972

Date: 23/05/2026

9% Overall Similarity

The combined total of all matches, including overlapping sources, for each database.

Filtered from the Report

- Bibliography
- Quoted Text
- Cited Text
- Small Matches (less than 10 words)

Match Groups

121 Not Cited or Quoted 9%
Matches with neither in-text citation nor quotation marks

0 Missing Quotations 0%
Matches that are still very similar to source material

0 Missing Citation 0%
Matches that have quotation marks, but no in-text citation

0 Cited and Quoted 0%
Matches with in-text citation present, but no quotation marks

Top Sources

7% Internet sources
7% Publications
5% Submitted works (Student Papers)

Integrity Flags

0 Integrity Flags for Review

Our system's algorithms look deeply at a document for any inconsistencies that would set it apart from a normal submission. If we notice something strange, we flag it for you to review.

A Flag is not necessarily an indicator of a problem. However, we'd recommend you focus your attention there for further review.

*% detected as AI

AI detection includes the possibility of false positives. Although some text in this submission is likely AI generated, scores below the 20% threshold are not surfaced because they have a higher likelihood of false positives.

Caution: Review required.

It is essential to understand the limitations of AI detection before making decisions about a student's work. We encourage you to learn more about Turnitin's AI detection capabilities before using the tool.

Disclaimer

Our AI writing assessment is designed to help educators identify text that might be prepared by a generative AI tool. Our AI writing assessment may not always be accurate (i.e., our AI models may produce either false positive results or false negative results), so it should not be used as the sole basis for adverse actions against a student. It takes further scrutiny and human judgment in conjunction with an organization's application of its specific academic policies to determine whether any academic misconduct has occurred.


DEPARTMENT OF MATHEMATICS
under the aegis of IRQAC
P.G.D.A.V. COLLEGE, UNIVERSITY OF DELHI
in association with
FACULTY OF MATHEMATICAL SCIENCES, UNIVERSITY OF DELHI
INDIAN INSTITUTE OF TECHNOLOGY (IIT), MANDI &
NATIONAL INSTITUTE OF TECHNOLOGY (NIT), UTTRAKHAND
ICMSCI-2026
INTERNATIONAL CONFERENCE ON MATHEMATICAL SCIENCES AND COMPUTATIONAL INTELLIGENCE
Certificate of Appreciation
This is to certify that
Mr. Sudhanshu Ranjan, Delhi Technological University
presented a research paper titled "Integral equation" at the International Conference on Mathematical Sciences and Computational Intelligence (ICMSCI-2026), held during 20-22 February, 2026, organized by Department of Mathematics, P.G.D.A.V. College, University of Delhi, in association with Faculty of Mathematical Sciences, University of Delhi, Indian Institute of Technology (IIT), Mandi & National Institute of Technology (NIT), Uttarakhand.
Prof. Darvinder Kumar
Principal
Dr. Shubham Jaiswal
Conference Chair & Convenor
Dr. Nav Shakti Mishra
Organizing Secretary
SPONSORS
Government Of India
Ministry of Statistics and Programme Implementation
Anusandhan National Research Foundation

Here is my abstract to present the paper in the upcoming conference

1 message

Sudhanshu Ranjan <sudhanshusrj00007@gmail.com> Thu, 30 Apr, 2026 at 11:29 pm
To: mmactvu@gmail.com

dissertation_abstract.pdf
121 KB

Registration link and paper ID

1 message

mmac tvu <mmactvu@gmail.com> Thu, 30 Apr, 2026 at 11:30 pm
To: Sudhanshu Ranjan <sudhanshusrj00007@gmail.com>

YOUR PAPER ID : RTCM231

Registration Link

Link : https://forms.gle/KLZyUpWiXNxuSbfo6

Next week will send the payment details

Dr. M. Syed Ali
Department of Mathematics,
Thiruvalluvar University, Vellore.

On Thu, Apr 30, 2026, 11:29 PM Sudhanshu Ranjan <sudhanshusrj00007@gmail.com> wrote: